Precise Leveling survey around mount Io, Kirishima Volcano (2012 - 2016)

*Takeshi Matsushima[1], Kazunari Uchida[1], Rintaro Miyamachi[1], Shiori Fujita[1], Manami Nakamoto[1], Hitoshi Y. Mori[2], Masayuki Murase[3], Takahiro Ohkura[4], Hiroyuki Inoue[4]

1.Institute of Seismology and Volcanology, Faculty of Science, Kyushu University, 2.Institute of Seismology and Volcanology, Faculty of Science, Hokkaido University, 3.Department of Geosystem Sciences, College of Humanities and Sciences, Nihon University, 4.Institute for Geothermal Sciences, Graduate School of Science, Kyoto University

Introduction

Since the magma eruption of Kirishima Shinmoedake in southern Kyushu in 2011, volcanic activity of the Kirishima mountain range had been followed by a calm situation.
However, the number of volcanic earthquakes is increased around Ebino plateau (Mount Io) a distance of about 5km northwest from Shinmoedake since December 2013.
In August 2014 occurred volcanic tremor that epicenter near mount Io and, it was also observed tilt change at the same time. Furthermore, geothermal field appeared in the summit area of Mount Io in December 2015, then also it began ejection of volcanic gas.
Mount Io is the vents of dacitic lava flow of 16 and 17th centuries in the eastern part of Ebino plateau. Although in the summit area had also been mining of sulfur up to 1962, in recent years it had declined rapidly its volcanic activity.
In the Kirishima volcanic area, level route has been established in 1968 by the University of Tokyo Earthquake Research Institute, and the phenomenon of subsidence and contraction of Mount Io have been observed in several times (Koyama et al., 1991). Ozawa et al. (2003) reported the local subsidence of Mount Io by using the interference SAR. We thought that activation of volcanic activity in the vicinity of Ebino plateau from the end of 2013 is a new magmatic activity, in order to understand the crustal deformation associated with this magma intrusion in detail, was carried out the leveling of near Ebino plateau.

Data and methods

Immediately after the eruption of Shinmoedake in 2011, Hokkaido University made a leveling of three times with about 25km section of Ebino city- Ebino plateau - Kirishima Shin'yu hot spring (Mori et al., 2012) . We carried out a re-measurement of about 8km section between Ebino plateu - Kirishima Shin'yu in June, 2015, and we have established a new route of about 2.5km in Mount Io direction. Also in 2015 December 19 to 22 we carried out to re-survey in the vicinity of Ebino plateau.

Result

With reference to the level point BM1120 level route western margin, the difference between the June measurement value and in December 2015 measured value at each level point are shown in the figure. Uplift amount is larger as it approaches the Mount Io from Ebino plateau (BM3015), uplift of up to 10.4 mm was recorded in west trailhead of Mount Io (BM3050). Uplift becomes gradually smaller when cross the mountain pass, and have returned to almost 0mm in BM3130 route northeast end.
Using the MaGCAP-V which the Meteorological Research Institute has developed, the elevation corrected Mogi model was determined by grid search. As a result, increasing pressure source of 3.1 $\times 10^4 m^3$ East 150m of Mount Io fumarole area, was estimated at an altitude of 600m. The vertical variation, which is calculated from this model is consistent with the crustal deformation observed by Earth Science and Disaster Prevention Research Institute using interference SAR analysis. The depth of the pressure source, which corresponds to the lower surface of the low-resistivity layer (impermeable layer) that has been estimated by Aizawa et al. (2013).

Keywords: Kirishima Volcano, Mount Io, Ebino Plateau, Precise Leveling Survey, Volcanic Ground Deformation

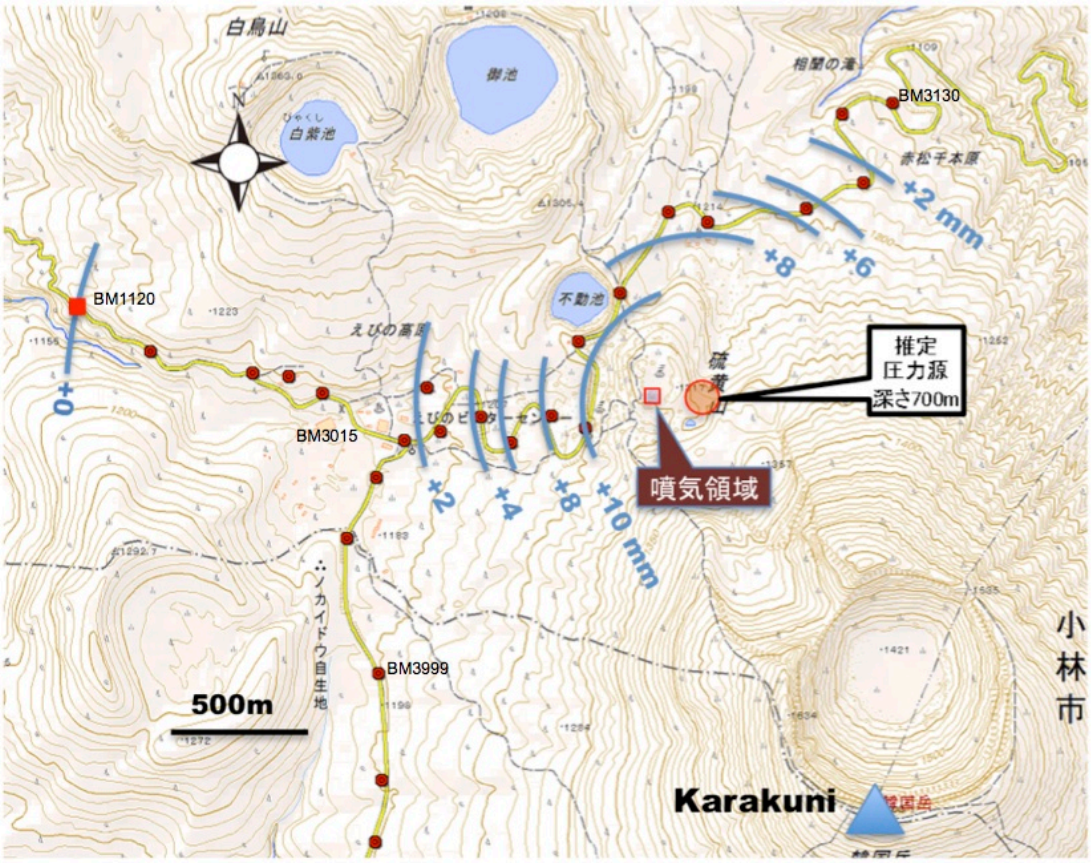

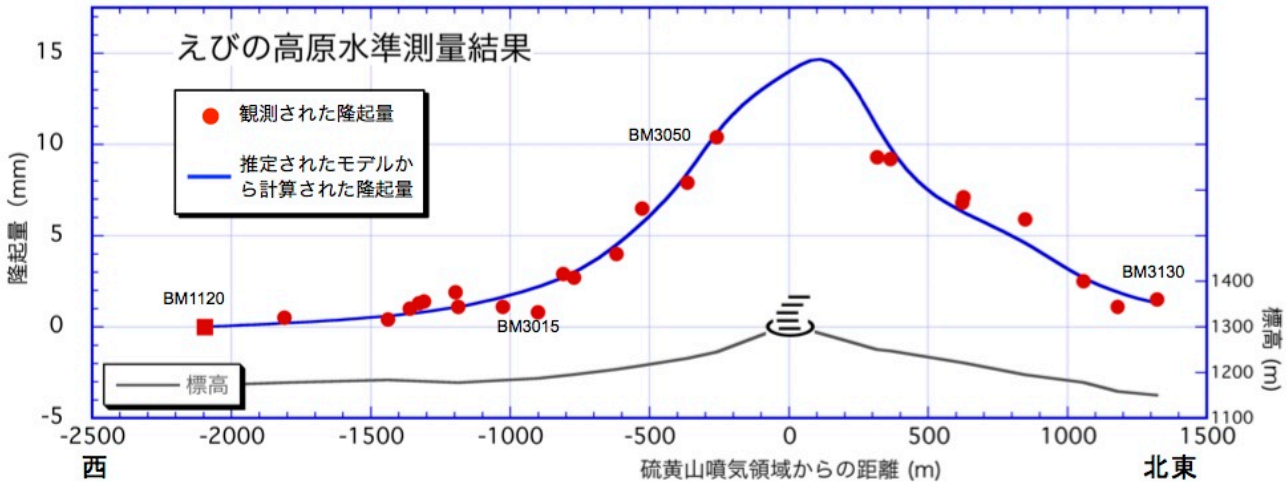

Probabilistic Prediction of Vulcanian Eruptions at the Showa Crater of Sakurajima Based on Ground Inflation

*Masato Iguchi[1]

1.Sakurajima Volcano Research Center, Disaster Prevention Research Institute, Kyoto University

Ground inflation was detected prior to 4422 vulcanian eruptions at Sakurajima by strainmenters. Frequency distributions of duration, amount, mean rate of strain change and ratio of inflation to deflation strain changes associated with eruptions show lognormal distribution. By using the lognormal distribution of the frequency as probability function, it is possible to stochastically forecast occurrence time and scale of the vulcanian eruptions.

Keywords: vulcanian eruption, precursory inflation, Probabilistic forecasting

Comparison between ground deformation events at Sakurajima from January to June 2015 and on August 15, 2015

*Kohei Hotta[1,2], Masato Iguchi[2], Takahiro Ohkura[1], Keigo Yamamoto[2], Takeshi Tameguri[2]

1.Graduate School of Science, Kyoto University, 2.DPRI, Kyoto University

We applied some source models to the ground deformations in different stages of volcanic activity of Sakurajima to make clear style and process of magma intrusion.
One is slow ground inflation with highly eruptive activity at the Showa crater during the period from January to June 2015 (first-half 2015 event). This event is similar to that during the period from October 2011 to March 2012 (2011 event). A pressure source analysis based on Mogi model (Mogi, 1958, BERI) during the 2011 event revealed inflation sources to be located at a depth of 9.6 km below sea level beneath the Aira caldera and 3.3 km below sea level beneath Kita-dake, and a deflation source is located at a depth of 0.7 km below sea level beneath Minami-dake (Hotta et al., 2016, JVGR). The characteristics of ground deformation during the first-half 2015 event is similar to that of the 2011 event, and inflation sources beneath Aira caldera and Kita-dake and a deflation source beneath Minami-dake are considered.
The other is much rapider and larger ground deformation on August 15, 2015, when eruptive activity was decreasing from July 2015 (August 2015 event). The pattern of horizontal displacement during the period from August 14 to 16, 2015 shows a WNW-ESE extension, which suggests a tensile fault. A nearly vertical dike with a strike of NNE-SSW is obtained at a depth of 1.0 km below sea level beneath Minami-dake. The length and width are 2.3 km and 0.6 km, respectively. The opening 1.97 m yields its volume increase +2.7 million cubic meters (Hotta et al., under revision, EPS).
Associated with the August 2015 event, 887 volcano-tectonic (VT) earthquakes occurred beside the dike, differently from the first-half 2015 event while only 63 VT earthquakes occurred for the 6 months. Half of the total amount of deformation of the August 2015 event was concentrated from 10:27 to 11:54. It is estimated that the intrusion rate of magma was 1 million cubic meters per hour during the period. This rate is 200 times larger than that of magma intrusion rate beneath Minami-dake prior to the vulcanian eruption on July 24, 2012 (5 thousand cubic meters per hour; Iguchi, 2013, Study on volcanic eruption process by multi-parameter observation at Sakurajima). The quite rapid intrusion rate caused extremely high-rate accumulation of strain in surrounding rocks, and this forced significant increase in seismicity. The first-half 2015 event is considered to be a process of magma accumulation and migration among the pre-existing spherical reservoirs, similarly to the previous activities such as the 2011 event. Conversely, the August 2015 event is dike-creating event at a different place from the pre-existing reservoir beneath the Showa crater, and magma stopped at a shallow depth of 1.0 km. The direction of the opening of the dike coincides with the T-axes of the VT earthquakes at the SW flank and is influenced by tectonic stress around the Sakurajima volcano. The VT earthquakes at the SW flank during the periods of 1976–1978 and 2003–2004 are inferred to be the magma pass from southwestern part of Sakurajima (Kamo, 1989, Proceedings of Kagoshima International Conference on Volcanoes) and vertical tensile crack that across Sakurajima from NE to SW (Hidayati et al., 2007, BVSJ), respectively. The first-half 2015 event was accompanied by the VT earthquakes at the SW flank during the period from March 31 to early April, 2015, similarly to 1976–1978 and 2003–2004. Magma might migrate beneath the dike intruded on the August 2015 event along the magma pass from southwestern part of Sakurajima or along vertical tensile crack that across Sakurajima from NE to SW accompany with the swarm of VT earthquakes at the southwestern part of Sakurajima in the first-half 2015 event.

Keywords: Sakurajima volcano, ground deformation, geodetic data, VT earthquake

Continuous relative gravity observation at Sakurajima Volcano: Tilt and gravity changes during the dike intrusion event

*Takahito Kazama[1], Keigo Yamamoto[2], Masato Iguchi[2]

1.Kyoto University, 2.DPRI, Kyoto University

At Sakurajima Volcano (Kagoshima Prefecture, Western Japan), rapid tilt changes due to the inflation of the mountain body were observed on 15 August 2015, along with the increase of volcanic earthquakes (Japan Meteorological Agency, 2015). Geodetic investigations also showed that the inflation was caused by the intrusion of a dike, whose strike direction was close to the north-south axis (Geospatial Information Authority of Japan, 2015). Ascending volcanic fluid may be related to the dike intrusion, but physical properties of the fluid such as density cannot be directly identified from the observations of earthquakes and crustal deformations because these observations only detect indirect deformations of the volcanic medium.
We thus utilize the minutely continuous data of relative gravity and tilts collected by a Scintrex CG-3M gravimeter at Arimura Observatory (2.1 km south-southeast of the Showa crater), in order to discuss the mass movement process during the dike intrusion event on 15 August 2015. Note that we already corrected several disturbances in the raw data of the gravity and tilts (such as the tidal effect and instrumental drift), which will be presented in the “Gravity and Geoid” session in detail.
Tilt change: The blue and green lines in the upper panel of the attached figure show the time variations in tilt for the N35E and N55W axes on 15 August 2015, respectively. Two tilt values increased rapidly around noon, suggesting that the ground uplifted at the north of Arimura Observatory (i.e., at the area of the volcanic craters). We estimated the time constant and amplitudes of the tilt variations by fitting the exponential functions of exp(x) for x<0 and 2 - exp(-x) for x>=0 through the trial-and-error approach. The peak-to-peak tilt amplitudes are +36 and +42 micro-rad for the N35E and N55W axes, respectively, so the absolute value of the tilt changes is calculated to be 56 micro-rad, which is about 65 % of that recorded in the Arimura tunnel (Japan Meteorological Agency, 2015). In addition, the time constant of the exponential functions is 1.0 hour, and the two tilt components varied most rapidly at 11:30 in JST.
Relative gravity change: The red lines in the lower panel of the attached figure show the relative gravity change in 15 August 2015, recorded by the CG-3M gravimeter. Although a part of the gravity data scatters due to the active seismicity, a gravity step can be identified in the instrumental drift with a period of a few days. By applying the regression of a fifth-order function and the above exponential function to the gravity time series, the peak-to-peak amplitude of the gravity step is calculated to be +9 micro-Gal. However, this gravity change is inconsistent with that observed by an absolute gravimeter at Arimura Observatory (-5 micro-Gal; Okubo et al., 2015) in terms of the sign and absolute amplitude. One of the possible reasons is that the relative gravity data was disturbed by apparent gravity changes due to the significant tilt changes. In our presentation, we will report the investigation results of the tilt-derived apparent gravity changes to discuss the mass movement process from the gravity signals associated with the dike intrusion.

Keywords: relative gravity, gravity change, tilt change, Sakurajima Volcano, dike, magma

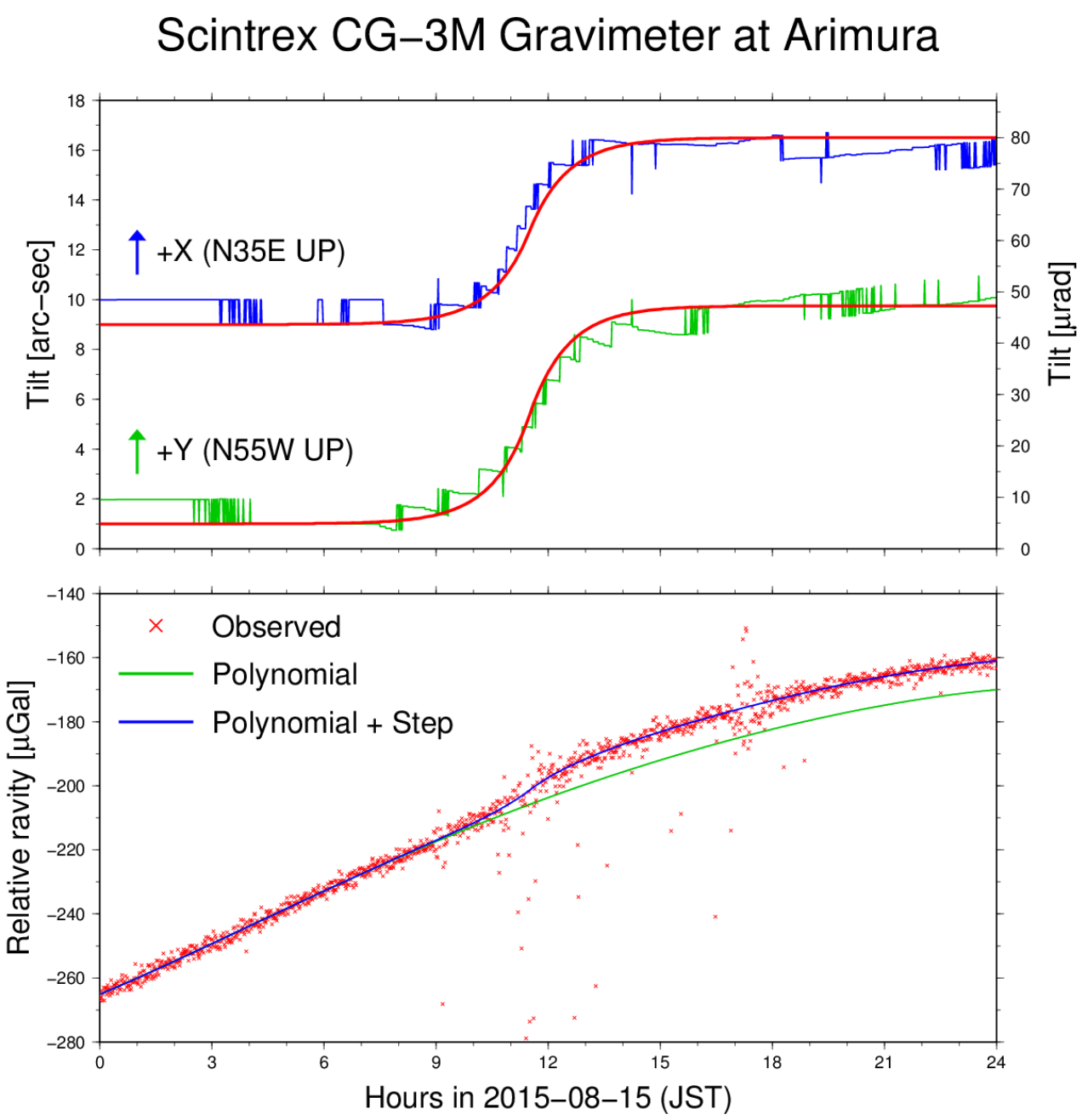

Gravity vs Strain/Tilt Changes at Sakurajima Volcano from the Dyke Intrusion Event in August 2015 through Resumption of Frequent Explosions in February 2016

*Shuhei Okubo[1], Keigo Yamamoto[2], Masato Iguchi[2], Yoshiyuki Tanaka[1], Yu Takagi[1]

1.Earthquake Research Institute, The University of Tokyo, 2.Disaster Prevention Research Institute, Kyoto University

In this paper, we deal with short-term gravity signals based on continuous absolute gravity measurements from July 2015 through February 2015. During this period, significant seismicity and crustal deformations were observed on Aug. 15, 2015, followed by unusual quiescence from late September 2015 through early February 2016.
We compared gravity $g(t)$ with strain or tilt record $e(t)$ on Sakurajima volcano. Two aspects are noteworthy to point out. That is,
(1) The ratio $| g(t) / e(t) |$ during the dyke intrusion (Aug. 15, 2015) is 100 times smaller than that during the other explosion period.
(2) Time lag between $g(t)$ and $e(t)$ is negligibly small during the dyke intrusion (Aug. 15, 2015) while $g(t)$ during the other period shows significant time lag (~1 day) to $e(t)$.
These characteristics are well explained in terms of the conduit status (open/closed). When the conduit is closed as in the case of the dyke intrusion event, both strain/tilt and gravity are principally governed by instantaneous elastic deformation, which implies absence of time lag. On the other hand, when the conduit is open as in the explosion period other than the dyke intrusion event, inflation/deflation of magma chamber does not cause effective elastic deformation, which means larger $|g(t) / e(t) |$ compared to the case of closed conduit and significant time lag of $g(t)$ to $e(t)$ because magma migration in a conduit requires certain amount of time.

Keywords: Gravity, Sakurajima, Magma Head, Crustal Deformation, Open Conduit, Vulcanian Eruption

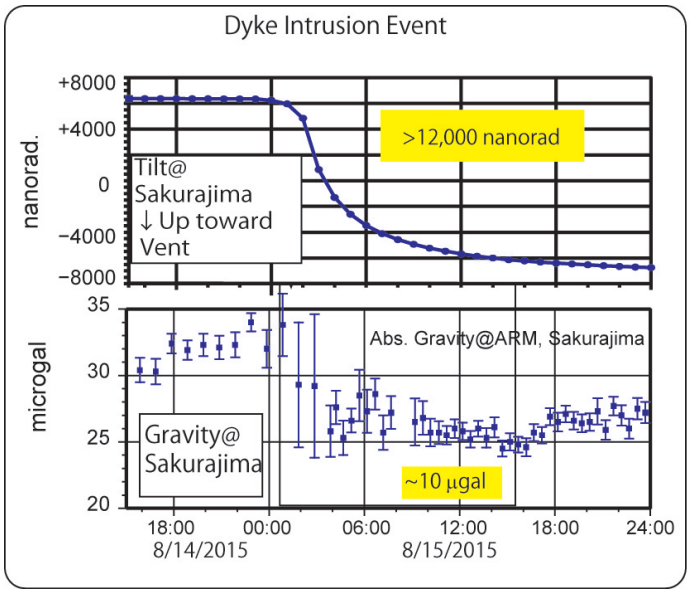

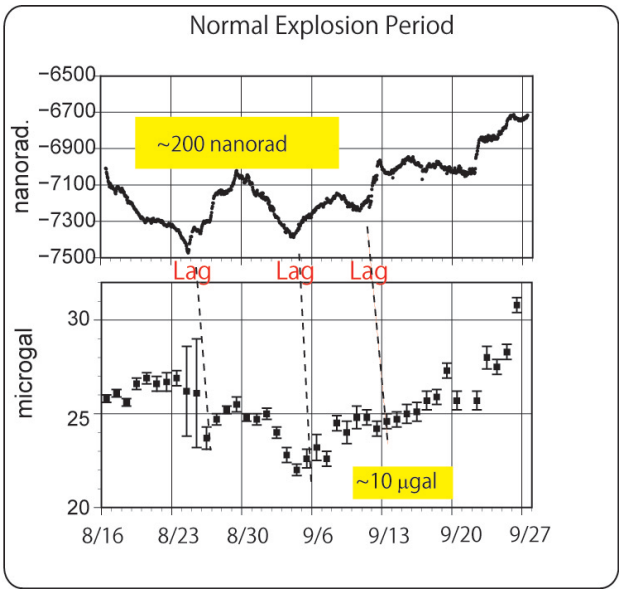

Vertical deformation associated with the 15 August 2015 dike intrusion at Sakurajima volcano measured by leveling survey

*Keigo Yamamoto[1], Shin Yoshikawa[2], Takeshi Matsushima[3], Takahiro Ohkura[2], Akihiko Yokoo[2], Hiroyuki Inoue[2], Kazunari Uchida[3], Tadaomi Sonoda[1], Manami Nakamoto[3], Yusuke Yamashita[1], Daisuke Miki[1], Satoshi Matsumoto[3], Koki Aizawa[3], Mie Ichihara[4]

1.Disaster Prevention Research Institute, Kyoto University, 2.Graduate School of Science, Kyoto University, 3.Faculty of Sciences, Kyushu University, 4.Earthquake Research Institute, University of Tokyo

We conducted the precise leveling survey in and around Sakurajima volcano, in order to detect the vertical ground deformation associated with the dike intrusion event occurred on August 15, 2015. The leveling routes measured in this survey are about 69 km long in total, including Sakurajima coast route, Sakurajima western flank route, Sakurajima northern flank route, Kurokami route in the eastern side of this volcano and Kagoshima Bay western coast route located outside Sakurajima. These leveling routes were measured during the periods from August 16 to September 24 and on December 18, 2015, immediately after the occurrence of the intrusion event. Mean square errors of the conducted survey were achieved with a good accuracy as the range from ±0.17 to ±0.33 mm/km. From the survey data measured in Sakurajima, we calculate the relative height of each bench mark referred to the reference bench mark BM.S.17 which is located at the western coast of Sakurajima. The calculated relative heights of the bench marks are then compared with those of the previous survey conducted in November 2014 (Yamamoto et al., 2015), resulting in the relative vertical displacements of the bench marks during the period from November 2014 to August-September 2015. As to the measured data of Kagoshima Bay western coast route, the reference bench mark is taken at BM.2469 located in Kagoshima city to the west of Sakurajima, and we calculate the relative vertical displacements of the bench marks during the period from November 2013 (when the previous survey was conducted in this route) to August 2015.
The resultant displacements indicate the remarkable ground uplifts around the northern part of Sakurajima, at Arimura (to the south of craters) and at Kurokami (to the east of craters). The amount of the maximum uplift is as much as about 16.8 mm referred to BM.S.17. The obtained uplifts at Arimura and Kurokami are consistent with the vertical ground deformation expected from the dike intrusion models inferred by other researches using InSAR, GNSS, tilt and strain data associated with the August 15 event (Geospatial Information Authority of Japan, 2015; Hotta et al., 2016). The uplifts around the northern part of Sakurajima suggest the inflation of the magma reservoir beneath the northern part of Sakurajima or beneath Aira caldera, which was not simultaneous with the August 15 event.

Keywords: Sakurajima volcano, dike intrusion, precise leveling survey, vertical ground deformation

Earthquake Swarm Activity at Sakurajima Volcano on August 15, 2015

*Takeshi Tameguri[1], Kohei Hotta[1], Masato Iguchi[1]

1.Sakurajima Volcano Research Center,Disaster Prevention Research Institute, Kyoto University

Explosive eruptions of vulcanian type have occurred at the summit crater Minamidake at Sakurajima volcano, Japan, since 1955. Principal eruptive activity shifted to the Showa crater at the eastern flank of the summit in 2006. The eruptions at the Showa crater were phreatic in 2006-2007 and vulcanian eruptions started from 2008. Minor vulcanian eruptions occurred about 500-1,000 times per year in 2010-2014. The eruptions occurred about 100 times every month until June in 2015. However, the eruptive activity gradually decreased from July. Active earthquake swarm and rapid ground deformation occurred on August 15, 2015 after decrease of the eruptive activity from July. In this study, we research temporary change of the earthquake activity, hypocenter distribution, source mechanism, and relationship the earthquake swarm between the rapid ground deformation.

The earthquake swarm are almost VT (Volcano-Tectonic) earthquake type, reached to 887 events on August 15. This swarm was obvious abnormal activity because the VT earthquakes occurred at most 40 events per month in Sakurajima. Location of hypocenters are calculated by using arrival times of P-wave first motion (more than 12 stations) and S-wave (more than 6 stations) assuming homogeneous half-space Vp=2.5km/s and Vp/Vs=1.73. Hypocenters are located beneath active craters Minamidake and Showa at depths 1.5 to 3.5 km. Source mechanisms determined using polarities of the first motions are normal fault (shallower than 2km) and strike slip types (deeper than 2km). The hypocenter location and source mechanism are similar pattern to general VT earthquake activities of the Sakurajima volcano (Hidayati et al., 2007, Bull. Volcanol. Soc. Japan).

Rapid and large ground deformation was also observed on August 15 accompanied with the earthquake swarm. Pattern of horizontal displacement showed extension to WNW-ESE, which suggested open of tensile crack by magma intrusion. A nearly vertical dike with strike of NNE-SSW was obtained at a depth of 1.0km beneath the Minamidake. Length and width of the dike were 2.3km and 0.6km, respectively. The dike opening was about 2m and its volume increased 2.7 million cubic meter (Hotta et al., submit to EPS).

The hypocenters of the VT earthquakes are close to opening of the dike estimated from ground deformation data. The earthquake swarm started at 07:05. Then, larger earthquake (M1.5 and M1.7) and the largest earthquake (M2.3) occurred at 09:03 and 10:47, respectively. The seismicity was increase during after the largest earthquake to before 12 a.m. The ground deformation was clear from 8 a.m. and inflation rate increased from 9 a.m. Half of the total amount of the inflation was going on 10:27 to 11:54 of the same time as the active seismicity. The inflation rate changed to decrease after 11:54. Two large low-frequency earthquakes (LF events) occurred at 11:32 and 11:43 before the change of inflation rate at 11:54. The decrease of the inflation rate may be related to the occurrence of the LF events. First motions of the LF events were compression (up and away from the summit crater in the vertical and radial components, respectively) at the all stations. We determined the source mechanism of the LF events by waveform inversion. The LF events were generated by isotropic expansion at the depth of 1.0km beneath the Minamidake crater. The hypocenter location and the first motions of the LF events were similar to those of explosion earthquakes accompanied with explosive eruptions from the Showa and Minamidake craters. However, the LF events are not accompanied with eruptions from the active craters. It is thought that the LF events were probably generated in closing magma system.

Keywords: Sakurajima Volcano, Earthquake Swarm

Failed eruption observed by seismic arrays during the Sakujirama volcano activity on Aug. 15, 2015.

*Eisuke Fujita[1], Hideki Ueda[1], Taku Ozawa[1], Yosuke Miyagi[1], Takahiro Miwa[1], Ryohei Kawaguchi[1]

1.National research Instituite for Earth science and Disaster prevention, Volcanic research department

NIED conducts seismic array obervation at two sites (north of Kitadake and Kurokami) in Sakurajima volcano from March 2015. Each array consists of nine 1Hz seismometers and 1 infrasonic sensor with 200Hz data loggers. We analyzed seismic data observed during the failed eruption on Aug. 15, 2015. The observed waveforms have significant characteristics as below: 1) P-arrival times at Kitadake-array leads 0.2s to those at Kurokami-array around 7:00. At 6:00 seismic signal is clear at Kitadake-array but not at Kuromami-array. 2) Rough estimates of epicenters are around east of Minamidake-Nakadake. 3) Waveforms at all stations of Kitadake-array are coherent, but at Kurokami-array, seismic stations at east of Nabeyama and others show different features. 4) Waveforms in 12:00 have lower frequency components. 6) LP vents have precursory high freuqency noises.
Temporal change of cross-correlation factors of these seismic waveforms indicate that there are three different periods, i.e., A: 6:00 - 10:30, B: 10:30 - 12:00, and C: 12:00 - 24:00. There are no familiy waves between these three periods. In A period, many family earthquakes were observed but not in B period. During C period, some pairs separated as long as hours have high cross-correlation factors. It is implicated that, in the A period, some similar fault slip occurred successively in the inital phase of dike intrusion, in the B period, VT events may suggest random fractures, and there occured some similar slips all around the intruded dike in the C period.

Keywords: Sakurajima, magma intrusion, VT earthquakes

Unknown later arrivals in cross-line shooting seismograms of the repeating seismic experiments in Sakurajima Volcano

*Tomoki Tsutsui[1], Takeshi Tameguri[2], Masato Iguchi[2], Haruhisa Nakamichi[2], hiromitsu oshima[3], Hiroshi Aoyama[3], Sadato Ueki[4], Mare Yamamoto[4], Kenji Nogami[5], Minoru Takeo[6], Takao Ohminato[6], Mie Ichihara[6], Jun Oikawa[6], Takao Koyama[6], Yuta Maeda[7], Takahiro Ohkura[2], Hiroshi Shimizu[8], Takeshi Matsushima[8], Hiroki Miyamachi[9], Reiji Kobayashi[9], Hiroshi Yakiwara[9]

1.Akita University, 2.Kyoto University, 3.Hokkaido University, 4.Tohoku University, 5.Tokyo Institute of Technology, 6.University of Tokyo, 7.Nagoya University, 8.Kyushu University, 9.Kagoshima University

Clear unknown later arrivals will be presented, which are detected through reconsideration on cross-line shooting seismograms in Sakurajima Volcano. The later arrivals are interpreted as PP reflections or PS conversions beneath eastern flank of Kitadake.

The repeating seismic experiments in Sakurajima Volcano has been conducted on every December since 2009 through 2014 (Tsutsui et al. 2010; 2011; 2012; 2013; 2014). The experiment includes two seismic profiles in the northern and the eastern Sakurajima, and fourteen or fifteen chemical shots have been recorded at over 250 temporary stations on each experiment. The active reflector "Alpha" at 5.8km below sea level has been reported as a result of the experiments, which is located in the northeastern part of Sakurajima. However, only a portion of the active reflector has been presented in the paper under processing, which locates just beneath the seismic line.

On the other hand, the cross-line shooting seismograms have been waiting for analysis. We have obtained sets of the cross-line shooting seismograms due to continuous recording over the shootings. We detected and interpreted some clear later arrivals in the cross-line shooting seismograms as followings;

A clear later arrival appears on 2.9 through 3 seconds in the eastern stations for northern shots and also in their reversed configuration, in the source distance range of 4.0 to 4.8 km. The arrival only appears in the seismograms corresponding to path passing through 2 km ENE of Kitadake summit. The arrival is interpreted as PP reflections because they appear high apparent velocity and also been found in reversed geometry of the station and the shot. A PP reflector at 4.7 to 4.8km below sea level gives well explanation on the arrival time. It is of interest that the modeled reflector is located in the south of the reflector "Alpha", and is shallower than "Alpha".

Moreover, other clear later arrival appears in seismograms in northern Sakurajima for the eastern shot, which appears about 5.2 s in the range 4.5 through 5.5 km. The arrival has high apparent velocity, disappears in the seismograms at the reversed geometry, and shows larger amplitude than that expected in PP arrival time. The arrival is interpreted to be PS conversion because of those above feature in seismograms. Assuming Vp/Vs is 1.73, the conversion at 5.8 km below sea level in NE of Kitadake can explain its travel time. It is significant that the converting points locate just at the same depth of the active reflector "Alpha", and locate between previous reflector and the reflection " Alpha" . Moreover, amplitude of the conversion has been changing through the seismic rounds.

Later arrivals have been detected in cross-line shooting seismograms on 2014 of which an association with the latest intrusion event on August 2015 is of interest.

Those seismic horizons beneath eastern to northeastern flank of Kitadake will be reported and their association with the intrusion event on August 2015 will be discussed.

Keywords: Volcanology, Sakurajima Volcano, Volcanic structure, Seismology

Depth of pre-eruptive magma reservoir of Sakurajima Volcano estimated from melt inclusions

*Naoki Araya[1], Michihiko Nakamura[1], Satoshi Okumura[1], Atsushi Yasuda[2], Daisuke Miki[3], Masato Iguchi[3]

1.Department of Earth Science, Graduate School of Science, Tohoku University, 2.Earthquake Research Institute, University of Tokyo, 3.Sakurajima Volcano Research Center, Disaster Prevention Research Institute, Kyoto University

To interprete magmatic processes of the ongoing Vulcanian explosions and to forecast possible future activity in Sakurajima Volcano, determining pre-eruptive magmatic conditions of the historic eruptions, especially depths of the magma reservoirs, is crucial. We therefore analyzed volatile contents and major element compositions of melt inclusions (MIs) and their host phenocrysts in the three historic Plinian eruptions (1471 A.D., 1779 A.D., and 1914 A.D.) and recent Vulcanian eruptions (1955-present).
The water contents of 110 MIs were analyzed with a FT-IR micro-reflectance spectroscopy (Yasuda, 2014). Most of the pyroxene-hosted melt inclusions (MIs) were dacitic to rhyolitic (SiO_2 = 65-72 wt.%) and gradually shifted to mafic compositions with time as observed for bulk rock compositions after the 1471 eruption (Uto et al., 2005; Nakagawa et al., 2011). The water contents of the MIs in the three historic Plinian eruptions have similar frequency distributions ranging from 1.2 to 3.5 wt.%. More than 95% of the data were within 1.2-2.9 wt.%. By contrast, those of melt inclusions in the recent Vulcanian ejecta were less than 2.3 wt.%. The lower maximum water content of the erupted materials of the Vulcanian explosions compared to those of the Plinian eruptions are interpreted as a result of degassing before quenching upon eruption. The MIs containing up to 40 ppm CO_2 were rarely found (Sato et al., 2012, JpGU), but most of the MIs did not contain detectable CO_2 content. The saturation pressure for the water content of 1.2-2.9 wt.% was calculated at 15-73 MPa, which corresponds to the depth of 0.6-3.1 km assuming that density of the upper crust is 2400 kg/m^3. The depth of the shallowest magma reservoir estimated from the geodetic observations on the present Vulcanian explosions are located at a depth of 4 km beneath the Minamidake summit (Iguchi et al., 2013), which is deeper than the depth ranges for most of the MIs (0.6-3.1 km) and in accordance with the maximum depth (4.1 km, corresponding to 3.5 wt% H_2O). Considering the erupted volumes of these Plinian eruptions (0.3-0.8 km^3 for the Plinian eruptions and 0.8-2.0 km^3 including lava flows in DRE, Kobayashi et al., 2013), the obtained depth range (2.5 km) may be largely explained by the difference in the position of the magma reservoir.

Keywords: Sakurajima Volcano, magma reservoir, melt inclusion, water content

Volcanic gas composition of Sakurajima volcano, Japan

*Hiroshi Shinohara[1], Ryunosuke KAZAHAYA[1], Urumu Tsunogai[2], Takao Ohminato[3], Takayuki Kaneko[3]

1.Geological Survey of Japan, AIST, 2.Graduate School of Environmental Studies, Nagoya University, 3.Earthquake Research Institute, University of Tokyo

We conducted volcanic gas composition measurements applying Multi-GAS and alkaline-filter techniques at Sakurajima volcano, which continues persistent degassing and frequent small-scale Vulcanian eruptions for several decades. The Multi-GAS and alkaline-filter needs to be conducted in a dense plume for precise measurement. However, we cannot access to the summit area of the volcano because of the frequent eruption and we applied various techniques to approach the volcanic plume at Sakurajima, including 1) air-borne measurement with a Cessna aircraft, 2) air-borne measurement with an unmanned helicopter and 3) automatic measurement at a flank of the volcano. Accuracy of the estimated gas composition depends on measured volcanic gas concentration which is quite variable depending on wind speed, direction, volcanic activity and distance from the summit crater.
We started the measurement in 2012. Until the early 2015, Sakurajima volcano continues the intensive persistent degassing with SO2 flux larger than 1,000 t/d and with frequent explosions at Showa crater, but SO2 flux decreased to around 100 t/d in the late 2015 with quite limited number of explosions. The volcanic gas compositions are fairly well estimated during the high flux period. The estimated average composition is; CO2/SO2 = 0.5, H2O/SO2=110, SO2/H2S=8, H2/SO2=0.15 and SO2/Cl=10 (mol ratio). This composition is similar to composition of other high-temperature gases in Japan with an exception of larger H2O/SO2 than others (i.e., about 40 at Asama, Miyake and Aso volcanoes). The CO2/SO2 ratios vary between 0.5-1.5 but negatively correlate with the measured SO2 concentration. The similar correlations observed at Asama volcano were interpreted as the results of mixing of low-temperature gases with low SO2 and high CO2 concentrations. At Sakurajima volcano, however, distribution of low-temperature fumaroles are limited and the cause of the correlation is not clear. The SO2/Cl ratios vary 5-20, which is consistent with the SO2/HCl ratios measured in 2009-2013 by FT-IR for the gas plume from the Showa crater (Mori et al., 2004).
During the low flux period in the late 2015 and the early 2016, the estimated ratios are different from those during the high flux periods; SO2/H2S=0.6-2.5 and CO2/SO2 = 20-150. During the low flux period, the measured gas concentrations were quite low (with maximum SO2 concentration of 0.1-0.5 ppm) and the estimated ratios are likely associated with quite large uncertainty, in particular for CO2/SO2 ratios. We measured d13C of CO2 in the plume samples collected during the flight when CO2/SO2 ratios were estimated as 150 and estimated the large CO2/SO2 ratio was caused by CO2 with low d13C (about -25 per mil) which is quite different from a common volcanic gas CO2 and the large ratio is unlikely represent that of the gases from the summit vent. The SO2/H2S ratios during the low flux period are lower than those during the high flux period. The low values can be caused by various reasons, however, most likely cause might be pressure difference of magma degassing. Since SO2/H2S ratio at constant oxygen fugacity and temperature inversely proportional to pressure, 10 times increase of the degassing pressure can cause the ten times decrease of the SO2/H2S ratios.

Keywords: Volcanic gas, volcanic plume, Sakurajima

Detection of abrupt increase in CO_2 flux from a submarine volcano, Wakamiko, in the innermost par of Kagoshima Bay in July 2015

*Toshiro Yamanaka[1], Kazuna Kondo[1], Mari Kobayashi[1], Takuro Noguchi[2], Kei Okamura[3], Tomoko Yamamoto[4], Urumu Tsunogai[5], Jun-ichiro Ishibashi[6]

1.Graduate School of Natural Science and Technology, Okayama University, 2.Multidisciplinary Science Cluster, Research and Education Faculty, Kochi University, 3.Center for Advanced Marine Core Research, Kochi University, 4.Faculty of Fisheries, Kagoshima University, 5.Graduate School of Environmental Studies, Nagoya University, 6.Graduate School of Science, Kyushu University

CO_2 flux from a submarine volcano, Wakamiko, Southern Kyushu, Japan, has been measured since 2007. The CO_2 flux from the volcano were varied ranging from 160 to 360 ton/day from 2007 to 2014, but in 2015 the flux is significantly increased up to 500 ton/day calculated using the data obtained in July. In the next month, August 2015, significant volcanic tremors were started beneath Sakurajima Volcano, so large-scale eruption of the volcano had been expected. After that, volcanic tremors beneath Sakurajima Volcano declined within two weeks, and also CO_2 flux from Wakamiko Volcano observed in December was decreased to similar range before 2014. Magma chamber beneath Aira Caldera has been considered to provide magmatic volatile to Wakamiko Volcano and to be connected with another shallower magma chamber beneath Sakurajima Volcano. The volcanic tremors were considered to be associated with ascending of magma from the shallower magma chamber. Therefore, the detected abrupt increase of CO_2 flux from Wakamiko Volcano may reflect those magma activities.

Keywords: Wakamiko submarine volcano, CO2 flux, Volcanic activity of Sakurajima Volcano

Hydrophone observations of volcanic activity from the sea area surrounding the Nishinoshima volcano

*Yozo Hamano[1], Hiroko Sugioka[2], Aki Ito[1], Mie Ichihara[3], Masanao Shinohara[3], Kiwamu Nishida[3], Minoru Takeo[3]

1.Department of Deep Earth Structure and Dynamics Research, JAMSTEC, 2.Department of Planetology, Kobe University, 3.Earthquake Research Institute, University of Tokyo

We develop a remote island volcano monitoring system using an autonomous sea-going platform (Sugioka et al. 2016). The system is planned to be capable of observing 1) volcanic eruptions with infrasound signals, 2) deep volcanic activity by seismic signals, 3) eruptive activity by photographs, and 4) ocean waves due to collapse of island slope. During the KR15-03 cruise of R/V KAIREI, we tested the performance of the sensors for these observations. And, five Ocean Bottom Seismometers (OBS) were deployed on the seafloor surrounding the Nishinoshima for more general purpose of monitoring the seismic activity around the volcano. Here, we report the results of the hydrophone observations, which is to be used for observing seismic activity of the volcano.
Hydrophone observation was made at the site 7km east to the Nishinoshima with water depth of 1318 m. The hydrophone was lowered from the ship to the depth of 10m below sea level. During the hydrophone measurements from 2015/2/27 13:20 to 14:40 (JST), videos of the volcano were taken continuously, and both the infrasound recorders on top of the ship and the OBS at the site NI11 14km east to the Nishinoshima were also operating. These simultaneous observations provide a big progress of understanding the role of each observation, and constructing a monitoring system of island volcanoes.
During the observation period, the volcanic activity was very high and eruptions with durations of 20 to 30 seconds occur with the frequency of about 15 events in ten minutes. The sequence of eruptions correlates well with the OBS and infrasound records, suggesting the seismic and infrasound signals are closely related to the eruptive activity at the shallow part of the volcanic body (Ichihara et al., 2016).
On the other hand, the features of hydrophone records are completely different. The most prominent feature of the hydrophone record is the harmonic tremor lasting about 20 minutes, which seem to be generated by deeper activities of the volcano. Underwater sound velocity structure seems responsible for that the wave sources for the OBS and the hydrophone are different. As for the sound velocity structure around the Nishinoshima estimated by the CTD measurement, the sound speed of surface 200 m is almost constant with the speed of 1518m/s. Below this depth, the sound speed drastically decreases to 1480 m/s at 1000m depth, and then slowly increase to 1490 m/s at 2000m depth. This sound speed structure suggests shadow zone at the sea surface depending on the source depth of the sound wave. Assuming that the position of the hydrophone is within the shadow zone, wave source of the explosion earthquakes is estimated to be deeper than 200m, but not much deeper than this depth, whereas the source depth of the harmonic tremor observed by the hydrophone seems to be as deep as 1300m, which is the water depth of the observation site of the hydrophone. It is not clear why the harmonic tremor is not recorded in the OBS. Probably, the T-phase signals are too large due to the low attenuation of the sound wave propagating through the underwater channel. The observation results explained above is extremely important for establishing the observation plan of the remote island volcano monitoring system.

Keywords: Nishinoshima, Volcanic activiy, Hydrophone observation

Multi-parametric observation for assessing activity of Nishinoshima volcano

*Mie Ichihara[1], Masanao Shinohara[1], Kiwamu Nishida[1], Shin'ichi Sakai[1], Tomoaki Yamada[1], Minoru Takeo[1], Hiroko Sugioka[5], Yozo Hamano[2], Yutaka Nagaoka[3], Akimichi Takagi[3], Taisei Morishita[4], Azusa Nishizawa[4]

1.Earthquake Research Institute, University of Tokyo, 2.JAMSTEC, 3.JMA, Meteorological Research Institute, 4.Japan Cost Guard, 5.Kobe University

Nishinoshima started eruptive activity in November, 2013, and a new island is created. Few observation data are available to assess the eruptive activity at such a remote island. This study is intended to get more information of the volcanic activity at Nishinoshima and to develop methods for monitoring remote island volcanoes. We conducted continuous recordings of infrasound at the nearest accessible island and of seismic waves with OBSs around Nishinoshima. We also took movies and infrasonic data during the installation of the OBSs. Here we report the results.
Observation:
The continuous infrasonic observation is conducted at Chichijima island about 130 km east of Nishinoshima. An infrasonic array has been operated offline since April 26, 2014, and another online station was added on October 5, 2014. An automatic analysis is run once a day to detect infrasound from Nishinoshima using data from the online infrasonic station and a nearby seismic station operated by JMA. The offline array data is used for more detailed analyses. Ray-tracing for infrasound propagation from Nishinoshima to the stations is conducted using the atmospheric data measured at Chichijima observatory of JMA. The result is used to evaluate the atmospheric effect.
Five OBSs were installed around Nishinoshima on February 27-28, 2015, during the KR15-03 cruise of R/V KAIREI (JAMSTEC), and retrieved on October 3-4 during the KS15-07 cruise of R/V KEIFU (JMA). The first OBS station (NI11) was installed about 13 km to the south-east of Nishinoshima. Then in the afternoon of February 27, the boat stayed to the east of Nishinoshima in the distance about 6 km, and the movies and infrasonic data were recorded. The other 4 OBS stations (NI21-NI51) were installed afterward around Nishinoshima in the distance about 7 km.
Results:
The movies are compared with the infrasonic data recorded on the boat and the seismic data recorded at NI11. The times of the infrasonic and seismic data are shifted forward considering the propagation time. The signals associated with eruptions are clear in the 1-7 Hz band of the infrasound and in the 4-8 Hz band in the seismic data. The movies show that ash emission occurs intermittently with a cluster of successive small explosions. The individual explosions generate impulsive infrasound and a spindle-shape seismic wave packet is observed associated with the ash emission.
The continuous data of the five OBSs from February 28 to October 3, is used to analyze the spindle-shape wave packets. The epicenters are estimated using the travel time differences for 15 events that occurred on February 28, and are determined around Nishinoshima. Such events are automatically detected by the STA/LTA method, and 363367 events are counted in the period. The occurrence changes in the mid July: the daily number starts decreasing and the duration of an event starts increasing. The maximum amplitude in an hour is small in March, grows from April to May, and then decreases. It seems growing again after the mid July.
The ray-tracing calculation shows that the atmospheric structure is good for the infrasound propagation only until the beginning of April, 2015. Few rays reach the station after June, and the change in mid July is not detectable, if any. In the latter half of May, there are some days when the atmospheric conditions allow the infrasound propagation to the station, but no signal is

detected. According to the OBS observation, Nishinoshima is seismically active in the period, as mentioned above.
The remote infrasonic observation can provide us with some information of the volcanic activity, but the atmospheric conditions do not always allow infrasound to reach the station from the volcano. Observation with OBSs installed close to the volcano is important. If we can at least obtain the results of such event analyses as presented above, the OBS observation would make a useful monitoring method.

Keywords: Volcano, Monitoring, Infrasound, OBS

Volcanic activity of the Nishinoshima volcano detected by ocean bottom seismometers and remote sensing observations

*Akimichi Takagi[1], Yutaka Nagaoka[1], Azusa Nishizawa[2], Tomozo Ono[2], Kenji Nakata[3], Kazuhiro Kimura[3], Keiichi Fukui[1], Shinobu Ando[3], Hiroaki Tsuchiyama[4]

1.Volcanology Research Department, Meteorological Research Institute, 2.Hydrographic and Oceanographic Department, Japan Coast Guard, 3.Seismology and Tsunami Research Department, Meteorological Research Institute, 4.Seismology and Volcanology Department, Japan Meteorological Agency

In order to detect seismic activity of the Nishinoshima Island volcano which continues to eruptions actively, the network of self-popup-type ocean-bottom seismometers (OBS) was deployed around the island by the Meteorological Research Institute. We report the brief summary of the seismic activity of Nishinoshima with reference to other remote sensing observations.
Five observation devices which have one three-component seismometer and one hydrophone were installed 4 - 5 km far from the center of Nishinoshima Island, and recorded seismic activity from June 12 to October 2, 2015. This observation revealed that micro-earthquake activity around Nishinoshima volcano was so active. Many micro earthquakes were estimated to be M -1 - 0. Duration time of waveform is around 30 seconds, and envelope of waveform is spindle shape without clear P and S phases. Initial part of waveform has high-frequency component. In later part, the low-frequency component is dominant. Hourly number of recorded waveform was 50 - 100 during the period of OBS. The number of waveforms was around 100 in June, 2015. But seismicity began to weaken in August, and then the number reached to 40 per hour in October. Amplitude of waveform has reached a large size gradually.
The gradual decrease trend of seismicity was consistent with variance of brightness temperature monitored by JMA's geostationary meteorological satellite Himawari-8 (JMA, 2016). In addition, though SO_2 flux in volcanic plume was measured to be 900 ton per day in May, 2015 by the Differential Optical Absorption Spectroscopy (DOAS), decreased to 400 ton per day in October, 2015. Moreover, heat flux of plume by optical sensor on the artificial satellite has decreased, and also incoherent area of the volcanic island by satellite SAR has decreased. So the gradual decrease trend of seismicity must have been synchronized to thermal and gas-emission activity in Nishinoshima volcano.
Another OBS network had been deployed around Nishinoshima from June 25 to July 5, 2015 by Japan Coast Guard (JCG). OBS station St5, located 8 km south far from Nishinoshima, detected active seismic swarms of monochromatic earthquakes. These waveforms have steep dominant frequency of 9 -10Hz, and decays slowly. All of waveform oscillations have same direction, and b value, estimated from frequency distribution of seismic scale, was calculated to be 1.3. St5, recorded these waveforms, was located near submarine volcano Nishinoshima-Minami Knoll. Around this area, discolored seawater and/or thermal anomaly were observed until now. Therefore this monochromatic-earthquakes swarm may have been recorded as an original volcanic activity different from Nishinoshima volcano.

Acknowledgment
Keifu Maru, the marine weather observation ship managed by Global Environment and Marine Department, JMA, was used for installation and pickup of OBS.

Keywords: Nishinoshima, ocean bottom seismometer, monochromatic earthquake, remote sensing

Development of a monitoring system of remote island volcanoes using an autonomous vehicle of the Wave Glider

*Hiroko Sugioka[1], Yozo Hamano[2], Mie Ichihara[3], Kiwamu Nishida[3], Minoru Takeo[3]

1.Kobe University, 2.JAMSTEC, 3.Earthquake Research Institute, University of Tokyo

Nishinoshima is a remote island volcano 1000 km south of Tokyo. On November 20, 2013, a brand new island was born nearby the older Nishinoshima. Over the past two years with continued volcanic activity, it has grown up to 12 times the size of the original island, which is offering us a rare opportunity to study how volcanic island forms and grows.
We develop a remote island volcanic activity monitoring system using an unmanned vehicle of the Wave Glider (WG), manufactured by Liquid Robotics Inc. of California, USA. The WG is designed to go forward using the wave and solar energy without any fuel and is equipped with a satellite communication modem to transmit data message to the land station in real-time. It has led the way to make ocean data collection and communications easier and safer, lower risk and cost, and real-time. In order to investigate the feasibility of the WG for station-keeping operation, we made a long-term deployment in the sea off Miyagi. Based on the detailed analyzing of 5 months navigation data from September to May in 2014, the potential utility of the WG as a sea surface gateway has been confirmed to identify the operating parameters.
In the remote island volcano monitoring system the WG plays roles not only in a satellite relay device but also in a multi-parametric observatory platform with microphones for detecting infrasound waves associated with volcanic eruptions, with hydrophones for detecting acoustic and seismic waves associated with deep volcanic activities, with wave gauges for detecting heave displacements associated with volcano collapse, and with video cameras. We investigated the performance of these sensors except for the wave gauge close to the Nishinoshima volcano during the KR15-03 cruise of R/V KAIREI in February 2015 (Hamano et al., 2016; Ichihara et al. 2016) and obtained extremely important results to establish the remote island volcano monitoring system.

Keywords: island volcanic activity, Nishinoshima, remote monitoring

Relative hypocenter determination of eruption earthquakes at Stromboli volcano based on a temporal observation in June 2015

*Shunsuke Sugimura[1], Takeshi Nishimura[1], Hiroshi Aoyama[2], Taishi Yamada[2], Ryohei Kawaguchi[3], Takahiro Miwa[3], Eisuke Fujita[3], Maurizio Ripepe[4], Riccardo Genco[4]

1.Graduate School of Science, Tohoku University, 2.Graduate School of Science, Hokkaido University, 3.NIED, 4.University of Florence

Earthquakes associated with eruptions of magma or gases are repeatedly observed with intervals of several or tens of minutes or hours on Strombolian explosions. The source of these earthquakes is likely the source of magma explosions associated with the rapid change of pressure in a conduit. Hypocenter determination of these eruption earthquakes enables us to understand the shape or location of the conduit. However, they generally have obscure onsets of P or S phases, which disable us to use general hypocenter determination methods using arrival times of these phases.
In our previous study, we developed a new relative hypocenter determination method using deconvolution and master event method (Sugimura et al., 2015, JpGU, VSJ). Deconvolution filter enables us to automatically obtain higher resolution of the arrival time difference between a master event and a slave event and to separate the arrivals of two or three explosion events occurring in a very short time. In June 2015, we developed a temporal seismic network at Stromboli volcano. In this study, we determine relative hypocenter locations of eruption earthquakes using our method and the temporal observation data.
In the observation, we deployed five short-period seismometers at 200 m-1 km from the crater at Stromboli volcano. To obtain higher accuracy of source locations, we deployed them at west of the crater or the lower altitude than the expected source. The signals were recorded with a sampling frequency of 250Hz (Kinkei System, EDR-X7000) or 200 Hz (Hakusan Kougyou, LS-8800). Observation period was about two days in the beginning of June 2015.
In addition to our data, we analyze the signals obtained by the two permanent broadband seismic stations of Department of Earth Sciences of the University of Florence. In our analysis, we use band pass filter for the signals at 0.2-0.4 Hz. We choose a master event and use deconvolution filter to obtain arrival time differences between the master event and the slave events. We further calculate time differences of the arrival time differences between two stations using cross correlation of the deconvoluted waveforms. This enables us to eliminate origin time differences and to express these time differences as linear functions of the relative source locations from the master event.
We assume ~200 m beneath SW crater for the master event and the wave velocity of 1000 m/s. The result shows that the relative source locations are distributed in the range of ~200m in depth and sub-vertically. In future, we will consider a more possible source location of a master event and compare the source of short-period signals to understand the mechanism of magma explosions in a conduit at Stromboli.

Keywords: hypocenter determination, eruption earthquake, deconvolution, Stromboli volcano

Seismicity model of volcanic earthquakes for a quantitative assessment of volcanic activity

*Yuichi Morita[1]

1.Earthquake Research Institute, University of Tokyo

The activity of volcanic earthquakes is one of the well-established indicators of volcanic activities and precursors to volcanic eruptions. An increasing seismicity is often followed by a volcanic eruption (e.g. Mt. Usu 2000, Mt. Ontake 2014 eruptions). The earthquakes are generated not only by the temporal change of stress field that is caused by magma intrusio6n and/or emplacement (e.g. Izu Oshima 1986, Miyake 2000 eruptions), but also by increasing pore pressure on pre-existing faults caused by upwelling volatiles emitted from magma (e.g. phreatic eruption at Hakone 2015). To utilize the seismicity for quantitative evaluations of volcanic activities, we need to discriminate the effect of pore pressure changes from stress changes. To realize a quantitative evaluation, we need a physical model of seismicity and apply it in real case, and asses the model by comparing the estimated and observed seismicity.
One of the models that can relate stress changes to seismicity is rate and state dependence friction (RSF) law proposed by Dieterich (1994). We have already presented that the seismicity at Izu-Oshima volcano well obey the RSF law under the temporally changing inflations and deflations of the volcanic edifice. To check its validity at other volcanoes, we analyze seismicity around the other volcanoes induced by the 2011 Tohoku great earthquake.
Just after the 2011 Tohoku great earthquake, induced seismicity were appeared around more than 20 volcanoes in Japan. The seismicity increased rapidly and then decreases gradually like the sequence of after-shocks that is well-known as Ohmori's law. We analyzed the seismicity around 3 volcanoes: Nikkoshirane, Hakone and Yake-dake, because many hypocenters were determined by JMA around these volcanoes. At the same time, we estimate stress field around them using GEONET daily position data provided by GIA, Japan. We calculate Coulomb stress from the data and applied it to the RSF law to get an expected seismicity. Then, we compare the expected seismicity to observed one. In this analysis, we suppose that the focal mechanisms of the earthquake swarms are coincide with the expecting ones inferred from the estimated stress field. The great earthquake made a large strain over Japan Islands, and the large after-slip is lasting still now. The earthquake swarm zones are affected by stress rate change as well as stress step generated by the great earthquake. The RSF law can realize the feature and the estimated seismicity well match with the observed one. From this analysis, we can conclude that the RSF law is acceptable model for volcanic earthquake. The parameters of RSF concerning the relation between the stress rate and seismicity are also estimated for each volcano from the decay time of seismicity.
In this presentation, we demonstrate that RSF law is applicable to the seismicity of volcanic earthquakes generated by temporal variations of stress field. The pore pressure change at hypocenter region results in the difference between observed seismicity and estimated one based on RSF law. Therefore, in the case that seismicity is much larger than the estimated one, the effect of the pore pressure is dominant. It represents that of rising volatile affects the fault surface and it is precursor to the eruption. Here, the results for three volcanoes are presented now and further study will be carried out at present.
Acknowledgements: We are grateful to JMA for providing earthquake catalogue, and also to GIA, Japan for providing GEONET data.

Keywords: volcanic earthquake, seismicity, stress response, rate and state dependence friction law

Fluid properties estimated from frequencies of LP events using the analytical formula for crack resonance frequencies

*Kimiko Taguchi[1], Hiroyuki Kumagai[1], Yuta Maeda[1]

1.Nagoya University Environmental Studies

The crack model has been considered as a model of the resonator at the source of long-period (LP) events, and fluid types and sizes of resonators are estimated by comparison between peak frequencies of the observed LP events and resonance frequencies of the crack model by numerical simulations. However, numerical simulations required an extensive computational time, which prevented the systematic comparison to identify the oscillation modes of observed peak frequencies. Therefore, it was difficult to constrain all parameters of the crack model. Recently, Maeda and Kumagai (GRL, 2013) proposed an analytical formula for the resonance frequencies of the crack model, and this formula enables the comparison in a simple and systematic way. In this study, we investigated the resonance modes of peak frequencies of the observed LP events based on the analytical formula to estimate the crack model parameters. We analyzed observed LP events with the method described below. (1) First, we take the ratio of the resonance frequencies calculated by the analytical formula. We vary the assumed mode in the denominator of the ratio from the lowest mode to higher mode. Then, this ratio is expressed by three parameters of the crack model, m (the oscillation mode in the numerator of the ratio), W/L (the ratio of crack width to length), and C (crack stiffness). Here, C is expressed as $C = 3(a/\alpha)^2(\rho_f/\rho_s)(L/d)$, where a is the sound speed of the fluid in the crack, $\alpha$is the P wave velocity of the solid, ρ_f and ρ_s are the densities of the fluid and solid, respectively, and d is the aperture of the crack. Next, we take the ratio of observed peak frequencies to the lowest one. By comparison of the frequency ratio between the analytical and observed ones varying the assumed mode in the denominator and W/L systematically, we estimate W/L and C that best explain the observed peak frequencies successively from the lowest one. (2) It is known that Q factor of the crack model strongly depends on α/a (Kumagai and Chouet, JGR, 2000). So we estimate α/a by comparison between synthetic and observed waveforms based on numerical simulations of the crack model. We analyzed two LP events based on the step (1) (2). These LP events were observed at Kusatsu-Shirane volcano on 11 August and 2 November 1992. Here we refer to the events on 11 August and 2 November as the events 1 and 2, respectively. We first analyzed the event 1, and four observed peak frequencies were explained. Then we found that the fluid in the crack was explained by a misty gas, and all parameters of the crack model were estimated. We analyzed the event 2 in the same way, and we found that the fluid in the crack was also a misty gas but the crack size was larger than that of the event 1. These results suggest that water vapor was supplied to the crack in an aquifer system by outgassing from magma, then water vapor was cooled to saturation temperature, so the crack was filled with a misty gas. The difference of the crack size between the event 1 and the event 2 suggests that the amount of water vapor supplied to the crack in the event 2 was larger than that in the event 1. In the previous study of Kumagai et al. (JGR, 2002), it was difficult to compare observed peak frequencies to resonance frequencies of the crack model, so crack parameters (W/L, L/d) and oscillation modes were assumed. But the method used in this study enables simple and systematic identification of the modes of observed peak frequencies, and all parameters of the crack model can be constrained.

Acoustic VLP signals accompanying the continuous ash emission following Vulcanian eruptions

*Taishi Yamada[1], Hiroshi Aoyama[1], Takeshi Nishimura[2], Masato Iguchi[3], Muhamad Hendrasto[4]

1.Graduate School of Science, Hokkaido University, 2.Graduate School of Science, Tohoku University, 3.DPRI, Kyoto University, 4.CVGHM

Acoustic observation of active volcanoes has been provided the considerable information to understand the source process of volcano explosions (e.g., Fee and Matoza, 2013). However, Very Long Period (VLP) signals of acoustic wave accompanying volcanic explosions are poorly understood.In 2012-2013, we have conducted broadband seismic and infrasound observations of Vulcanian eruptions at Lokon-Empung volcano in Indonesia. The temporal observation network consists of 4 broadband seismometers (Trillium 40, Nanometrics Inc., 0.025-50 Hz) and an infrasound microphone (SI 102, Hakusan Co., 0.05-1500 Hz). About 80 % of observed vulcanian explosions are followed by the continuous ash emissions, which is recognized as the vibration in the seismic and infrasound waveforms. We find a VLP phase at the onset of the vibration in the band pass (0.03-0.1 Hz) vertical displacement waveforms and 0.1 Hz low pass pressure waveform. The apparent propagation velocity of the VLP phase at each station can be explained by the sound velocity near the ground from the vent. Hence, it is regarded that the VLP phase is induced by the acoustic wave accompanying the continuous ash emission. We analyze the broadband seismic data because the signals that have the period longer than 20 s (out of range of the flat pressure response of the microphone) dominate the band pass ground displacement waveforms.Similar VLP signals accompanying the continuous emission following the Vulcanian eruption can be seen in the broadband seismic records at Shinmoedake volcano in Japan in 2011. National research Institute for Earth science and Disaster prevention (NIED) has operated two broadband seismometers (Trillium 240, Nanometrics Inc., 0.004-200 Hz) and two barometers (AP270, Koshin Co.) near the active vent during the period of the activity of Shinmoedake in 2011. Seismic waveforms of Vulcanian eruptions on Jan. 27, 2011 show the explosive signals accompanying theexplosion and subsequent tremor induced by the continuous ash emission. Two infrasound microphones operated by Japan Meteorological Association (JMA) also recorded the signals associated with continuous ash emission after the explosion. We see the VLP phase propagating from the vent with the sound velocity accompanying the ash emission in the band pass (0.01-0.05 Hz) vertical displacement waveforms. The pressure change similar to the VLP phase is seen from the filtered (0.01-0.05 Hz) pressure waveforms recorded by the barometers.The maximum amplitude of vertical velocity of the VLP phase at both Lokon-Empung and Shinmoedake is in order of 10^{-7} m/s at 2-5000 m from the vent. The vertical velocity of the ground induced by the pressure change in the atmosphere is given by Ben-Menahem and Singh (1981). If we set the P-wave velocity and density of the ground as 2700 m/s and 2500 kg/m^3 as tentative values, we obtain the pressure change inducing the VLP phase at each station is in order of the 10^1 Pa. Since the signals having the wavelength about 10^3 m constitutes of the VLP phase, we can assume that the VLP phase can be excited by the point source at the vent and propagates as a linear sound wave. Based on this assumption, we can estimate the rate of mass outflow of the atmosphere (Lighthill, 2001) at the source. With the dry-air density in the atmosphere (1 kg/m^3), we estimate the mass flow rate of atmosphere in order of the 10^5 m^3/s. Although this estimation includes the effects of the amplification factor of the stations and wind noise, it is consistent to the mass flow rate of Vulcanian eruptions reported by the previous works (e.g., Koyaguchi, 2008). Therefore, the excitation of the VLP phase can be explained by the pressure change accompanying the formation of the ash column. Further investigation of the VLP phase can contribute to understand the dynamics of

the ash column and source process of Vulcanian eruptions.

Keywords: Ash column, Vulcanian eruptions, Infrasound

Active source seismic experiment in Zao Volcano, Japan

*Mare Yamamoto[1], Satoshi Miura[1], Masahiro Ichiki[1], Hiroshi Aoyama[2], Tomoki Tsutsui[3], Kentaro Emoto[1], Satoshi Hirahara[1], Takashi NAKAYAMA[1], Tatsuya Torimoto[1], Takao Ohminato[4], Atsushi Watanabe[4], Miwako Ando[4], Yuta Maeda[5], Takeshi Matsushima[6], Manami Nakamoto[6], Rintaro Miyamachi[6], Takahiro Ohkura[7], Shin Yoshikawa[7], Hiroki Miyamachi[8], Hiroaki Yanagisawa[9], Shinya Nagato[9]

1.Tohoku University, 2.Hokkaido University, 3.Akita University, 4.University of Tokyo, 5.Nagoya University, 6.Kyushu University, 7.Kyoto University, 8.Kagoshima University, 9.Japan Meteorological Agancy

Zao volcano is a Quaternary stratovolcano located in the central part of the volcanic front of the northeastern Japan. The most recent activity of Zao volcano began at ca. 35 ka at the central part of the volcano, and many historic eruptive activities including occurrence of lahar from the crater lake named Okama have been documented. After the occurrence of the 2011 Tohoku Earthquake, the activities of both deep low-frequency earthquakes and shallow long-period events beneath Zao volcano become higher, and it is thus important to reveal the subsurface structure and fluid distribution to prepare against possible future eruptive activities. With this point of view, as a part of MEXT 'Earthquake and Volcano Hazards Observation and Research Program', we conducted an active source experiment in October, 2015.
In the experiment, 132 temporal seismic stations were deployed on and around the volcano by 21 researchers from 8 universities and JMA, and seismic waves excited by two underground dynamite shots whose charges were 200 kg and 300 kg were recorded at a sampling frequency of 500 Hz. The configuration of seismic network was designed for refraction and fan-shooting analyses. In addition to these underground shots, to enhance the resolution of shallowmost structure, we also utilized a dynamite shot at a nearby quarrying plant, which generate surface waves suitable for the surface wave dispersion analysis.
As the first step of our analysis, we manually pick the arrival time of first onset at each station, and estimate velocity and depth of the basement layer by analyzing the obtained travel-time curves. By applying the time-term method, the P wave velocity of the basement is estimated as 5.2-5.5 km/s. An interesting point of this analysis is that the depth of the basement is quite shallow and at a depth of around 0.5 km from the ground surface. Although the uncertainty of this depth is still remaining, the result of surface wave dispersion analysis also supports the existence of basement at a shallow depth. We then apply the fan-shooting analysis to elucidate the distribution and extent of shallow hydrothermal system. From this analysis, we reveal that an attenuative zone seems to exist beneath slightly northeast of Okama at a depth of around 1 km.
In the previous studies, the subsurface structure of Zao volcano has been discussed mainly based on the geological observations. The results of the active seismic experiment such as the existence of shallow basement are consistent with these previous studies, and provide more detailed images of the subsurface structure beneath the volcano. Further studies including the relocation of volcanic earthquakes and elucidation of hydrothermal system may contribute to a better understanding of volcanic activities at Zao volcano.

Keywords: Zao Volcano, Active seismic experiment, Volcanic structure

Estimation of the low velocity region beneath Mt. Fuji revealed by inversion of receiver functions

*Sawako Kinoshita[1], Kiwamu Nishida[1], Toshihiro Igarashi[1], Yosuke Aoki[1], Minoru Takeo[1], Hideki Ueda[2]

1.Earthquake Research Institute, University of Tokyo, 2.National Research Institute for Earth Science and Disaster Prevention

Mt. Fuji, the largest stratovolcano in central Japan, has ejected a huge amount of basaltic products during the last 100,000 years. Although the reason for this high eruptive rate has not been well understood yet, a complicated tectonic setting is likely to be responsible for this uniqueness. Because the Izu-Bonin-Mariana arc (IBM) with a thickened crust is colliding and subducting below the Eurasian and Okhotsk plates around Mt. Fuji, a generic magma plumbing model for arc volcanoes is not readily applicable.
In this study, we conduct a receiver function (RF) analysis to investigate the seismic structure around Mt. Fuji including the distributions of the subducting IBM and the magma chamber below Mt. Fuji.
Cross sections of radial RF amplitudes reveal distinct positive velocity boundaries at depths of 40–60 km and 20–30 km around Mt. Fuji. We interpret the velocity boundary at 40–60 km depth as the lower boundary of the crust of IBM and that at 20–30 km depth as the lower boundary of the magma chamber of Mt. Fuji. Also, the velocity boundary representing the lower boundary of IBM crust does not continue just below Mt. Fuji at a depth of about 50 km, representing a locally weakened velocity contrast.
Next, we conducted an inversion analysis of receiver functions to investigate absolute S-wave velocities around Mt. Fuji, because the thick volcanic sediment layer and low velocity layers below Mt. Fuji change the amplitude of radial RFs. In RF inversions, there is a trade-off between the depth of the velocity boundary and the average velocity over the boundary, so we constrained results of the inversion by inverting receiver functions and dispersion curves of surface waves together. Our results are characterized by the following three features: 1) The north-south cross section of absolute velocities reveals that the width of IBM crust is developed down to a depth about 40 km. 2) Subducting oceanic crust, about 30–100 km to the southwest and 60–100 km to the northeast of Mt. Fuji, is represented by a low velocity body. 3) A distinct low velocity region exists below Mt. Fuji with a width of 40 km in horizontal direction and 20 km width in vertical direction, representing a crustal magma chamber of Mt. Fuji.
Our findings suggest that 1) Mt. Fuji has ejected mostly basaltic rocks because the crustal magma chamber is deep, and 2) an anomalously high eruption rate of Mt Fuji is because it hosts a large crustal magma chamber.

Keywords: Mt. Fuji, Receiver functions, Izu-Bonin-Mariana arc

Characteristics of seismic velocity changes on volcanoes using noise correlation method: Analyses of JMA seismic data

*Tomoya Takano[1], Takeshi Nishimura[1], Hisashi Nakahara[1]

1.Graduate School of Science, Tohoku University

Temporal changes of seismic velocity have been detected associated with the occurrence of large earthquakes and volcanic activities. The velocity changes are estimated to be about 0.1 ~ a few %. At active volcanoes, such seismic velocity changes are interpreted to be caused by the magma intrusion. To estimate seismic velocity changes preceding eruptions, it is important to examine the characteristic of seismic velocity changes during time periods having no volcanic activities. Therefore, we systematically investigate the characteristic of seismic velocity changes by applying seismic interferometry to ambient noise recorded at active volcanoes in Japan.
We estimate seismic velocity changes using continuous records of short period seismometers by Japan Meteorological Agency (JMA). We analyze 12 volcanoes which are observed by more than two seismometers and more than three GNSS stations: Hokkaido-Koma, Meakandake, Tokachidake, Tarumaesan, Adatarayama, Nasudake, Kusatsu-Shirane, Izuoshima, Miyakejima, Unzendake, Bandaisan, and Sakurajima. We use data from 2012 to 2013. Distances between stations are within about 5 km, and the number of station pairs ranges from 1 to 45 at each volcano. The seismic data are first filtered at 0.5-1Hz, 1-2Hz, and 2-4Hz, and cross correlation functions (CCF) of ambient seismic noise are then calculated. Daily seismic velocity changes are estimated by comparing each 1-day stacked CCF with a whole period stacked CCF as a reference based on MWCS method (Poupinet et al., 1984).
We recognize annual or a few monthly seismic velocity changes with amplitudes of about 1 ~ 3 %. The seismic velocity change largely even when there is no volcanic activity or earthquake. Correlation coefficients of velocity changes between each station pair at Izuoshima and Miyakejima and Tarumasan are high in the 1-2 Hz, however coefficients of other volcanoes are less than 0.5. The result implies that there would be localized velocity changes within the limits of a few kilometers in many volcanoes. We also compare seismic velocity changes between the three frequency bands for the same station pair. At a few volcanoes, the amplitudes of seismic velocity change are different between frequency bands while time series of velocity changes are well correlated. At the other volcanoes, trends or phases of seismic velocity changes are different. These results suggest changes of seismic velocity with depth or complex wave properties of ambient noise.
We investigate the relationship between seismic velocity changes and strain changes at each volcano because some studies reported velocity changes associated with stress changes. We estimate areal strain changes using three GNSS stations operated by JMA. We analyze the data with areal strain amplitudes of more than 2×10^{-6} and those of less than -2×10^{-6} considering measurement errors. We calculate the correlation coefficient between seismic velocity changes and areal strain changes using only time periods when the areal strain exceed the maximum shear strain. The high correlation coefficient between areal strain and seismic velocity changes are estimated at Izuoshima and Tarumaesan. However, it doesn't appear that seismic velocity changes correlate with areal strain changes in Tokachidake where irregular patterns are recognized in seismic velocity changes at three frequency bands and at different station pairs.
Seismic velocity changes are estimated to be about 1 ~ 3 % at volcanoes during no eruptive periods. Some stations show the high correlation coefficient between areal strain and seismic velocity changes. We suggest that areal strain changes may affect seismic velocity changes.

Keywords: Seismic velocity changes, Seismic interferometry, Volcano deformation

Shallow crustal velocity structures obtained from ambient noise study of dense broadband seismic array in the Tatun Volcano Group of Taiwan

*Yu-Chih Huang[1], Tsuneomi Kagiyama[1], Cheng-Horng Lin[2,3]

1.Aso Volcanological Laboratory, Institute of Geothermal Sciences, Graduate School of Science, Kyoto University, Kumamoto, Japan, 2.Institute of Earth Sciences, Academia Sinica, Taipei, Taiwan, 3.Taiwan Volcano Observatory at Tatun, Ministry of Science and Technology, Taipei, Taiwan

The Tatun Volcano Group (TVG) is located in the northern tip of Taiwan Island with a radius of 10 km. The TVG situates adjacent to the Taipei metropolis in the north and was predominantly active in the Quaternary period. Shanchiao Fault is an active normal fault transits the TVG in northeastern orientation. A sequence of normal faults and scarps inspected on the hanging wall of Shanchiao Fault and sub-parallel to its orientation in the extent of TVG. Since the major geothermal activities such as fumaroles, solfataras and hot springs also expose on the hanging wall of the Shanchiao Fault, it is thought to be the passage for volcanic-hydrothermal gas and fluid. Besides, Kanchiao Fault is a suspected active fault and known as the important geologic structures adjacent to the southeast of TVG.
The subjects about TVG is already extinct or still active are also under frequent discussion. Attribute to new technological advances and methodologies improvement, various types of observations and experiments were implemented to monitor the activities of TVG in recent years. Basing on the results of these recent researches, various evidence proved that TVG is not extinct, should be a potentially active volcano and cannot exclude the possibility of volcanic eruptions in the future. It is important to understand the magma chamber and detailed velocity structures below the TVG but are still not well resolved. The fundamental theory to obtain S-wave velocity structure from ambient seismic noise analysis has been already proofed and provided important constraints around the world in the past decade. We present the results of ambient seismic noise studies in the TVG with dense seismic monitoring network.
The seismic network in this research is composed with three sub-networks, totally there are 40 free-field seismic stations equipped with Güralp CMG-6TD broadband seismometers and GPS timing system. The interstation distances are between 0.6 km and 28 km, with an average of 8.5 km. The cross-correlation functions (CCFs) were calculated with the methodologies of one-bit cross-correlation and spectral whitening. We selected vertical component to obtain the CCFs in the period band 0.5-7 s for all station-pairs and derived with the selected daily recordings in 2014. The daily CCFs were stacked monthly and then the monthly CCFs were stacked again to further obtain TDEGFs and Rayleigh wave phase velocity dispersion curves. We stacked positive and negative lag times of TDEGF to enhance coherent signals and suppress the effect of uneven seismic noise sources distribution. The maximum period can be measured for each station-pair is related to the inter-station distance and phase velocity. For far-field approximation, the inter-station distance is required to be at least twice of propagating surface wave wavelengths in this study to assure surface wave can well develop between station-pair.
We focus on phase velocity maps in the period band 0.5-3 s in the TVG and the study region is parameterized by 0.02°×0.02° grid points. Phase velocity maps show high velocities are dominate between Shanchiao Fault and Kanchiao Fault at study periods, which maybe relate to the solidified andesite lava. Especially in the south parts of Jinshan area, which locates the earliest stage of volcanic activities in the TVG. At periods longer than 2.5 s, high velocities separate into two major regions beneath the ChiShingShan and south parts of Jinshan area. At periods shorter than 1 s, there are some localized low velocity areas correlate well with the surface geothermal

activities. The regions north (footwall) of Shanchiao Fault show low velocities at the study periods maybe relate to the Tertiary strata already covered by andesite lava flows with dozens of meters thickness. The detailed S-wave velocity structures in the shallow crust will be investigated and searching for possible candidates of magma passages and hydrothermal reservoirs beneath TVG.

Keywords: ambient seismic noise tomography, Tatun Volcano Group, shallow crust

Monitoring eruption activity using temporal stress changes at Mount Ontake volcano

*Toshiko Terakawa[1], Aitaro Kato[1], Yuta Maeda[1], Yoshiko Yamanaka[1], Shinichiro Horikawa[1], Kenjiro Matsuhiro[1], Takashi OKUDA[1]

1.Earthquake and Volcano Research Center, Graduate School of Environmental Studies, Nagoya University

On 27 September 2014, around 11:52 a.m. JST, Mt. Ontake volcano produced a hydrothermal eruption with a VEI value of 2. We examined temporal changes in the local stress field at Mt. Ontake over a period of 17 months (August 2014 to December 2015) with the 2014 eruption from focal mechanism solutions of 168 volcano-tectonic (VT) events (Terakawa et al., in press). In general, the local stress field around volcanoes represents the superposition of the regional stress field caused by plate motion and stress perturbation related to volcanic activity. The regional stress field does not change over periods of weeks to months, and so temporal stress changes over such time periods are attributed to volcanic activity.
We defined the angular difference between the observed slip vectors and theoretical slip vectors expected from the regional stress field as the misfit angle, based on the concept that seismic slip occurs in the direction of the resolved shear traction acting on a pre-existing fault. The misfit angles larger than the estimation errors of the regional stress field and focal mechanism solutions (>65°) mean that the local stress field was deviated from the regional stress field due to enhanced volcanic activity. The average misfit angles remarkably exceeded the threshold value (65°) two weeks before the eruption, but immediately after the eruption the values showed a marked decrease. The pre-eruption seismicity was dominated by normal faulting with ENE-WSW tension, indicating that the volcanic activity caused strong tension for the pre-eruption period. On the other hand, many reverse faulting with ESE-WNW compression for the post-eruption period corresponded to shrinkage of the volcanic edifice, controlled by the regional stress field.
The stress perturbation for the pre-eruption period suggests existence of dyke-type volcanic system beneath Mt. Ontake in which inflation is driven by magmatic/hydrothermal fluids propagating upwards in a vertical crack. This is consistent with the distribution of hypocenters of volcanic earthquakes relocated by a DD method (Kato et al., 2015), the alignment of craters from the 2014 eruption (GSI, 2014), and source mechanisms of VLP events prior to the 2007 and 2014 eruptions (Nakamichi et al., 2009, Maeda et al., 2015).
The time history of average misfit angles showed slight enhancements in November 2014, January-February 2015, June-July 2015, and October-December 2015. Especially, the final stage of the enhancement in June-July 2015 was synchronized with an unusual tiltmeter signal indicating summit upheaval. These observations suggest that some re-pressurization/de-pressurization processes repeated after the 2014 eruption. Temporal stress changes revealed in this study were well associated with physical processes at the active volcano. This indicates that the method has potential to contribute to eruption monitoring.

Keywords: Mount Ontake, stress fields, focal mechanism solutions

Deflation source after the September 2014 eruption of Ontake Volcano, Japan detected by ALOS2/PAlSAR2 InSAR

*Shohei Narita[1], Makoto MURAKAMI[1]

1.Institute of Seismology and Volcanology, Hokkaido Univ.

1. Introduction
On September 27th, a phreatic eruption occurred at Mt.Ontake, located on the border between Gifu and Nagano prefectures, central Japan. Preceding this event, the number of VT earthquakes gradually increased from early September, and their source was approaching ground surface during the final 10 minutes before the eruption. Simultaneously, the tilt meter located on the southeast flank recorded a rapid change suggesting inflation of the edifice. The eruption started on new eruptive fissures formed in Jigokudani, where there are many fumaroles and fissures formed in 1977. These activities then exponentially declined.
Multiple observations during the event suggest formation of co-eruptive crack just beneath Jigokudani area. Analysis of VLP event just before the eruption suggested that co-eruptive small crack opened at the depth of 300-1000m beneath the newly former fissures, and its orientation was approximately east-west (Maeda et al.,2015). ALOS2-InSAR detected co-eruptive ground deformation, revealing that co-eruptive crack aligned along new fissures extends vertically downward from 100m to 1400m (GSI, 2015). On the other hand, deflation around Jigokudani area after the eruption is confirmed by ALSO2 InSAR. The goal of this study is to reveal the source causing the deflation and its relationship to pressure sources during pre and co eruptive stages of 2014 eruption.
2. Data and Results
We processed 3 scenes of ALOS-2 data and computed 3 interferograms spanning 2014/10/03-2015/06/12 (8 month), 2014/10/03-2015/11/13 (13 month), 2015/06/12-2015/11/13 (5 month), respectively. All the interferograms were made from ascending and right looking observations having the same offnadir angle (32.4°). Coherency of those interferograms is very good. We used RINC 0.36version developed by Dr. Taku Ozawa at NIED.
In all the interferograms we detected LOS increase in the area of 2km×1km around Jigokudani. The distance changes in LOS direction mean subsidence, and its maximum values are respectively 45cm in 13month, 30cm in 8 month, and 12cm in 5 month. To estimate the source parameters causing the deformation, we carried out an inversion using Mogi model, which assumes point source buried in an elastic half-space. The depth of estimated sources is consistently about 400m beneath Jigokudani area. The volume changes are respectively $3.7\times10^5m^3$ in 13 month, $2.4\times10^5m^3$ in 8 month, $1.1\times10^5m^3$ in 5 month.
3. Discussions and future challenges
The deflating source estimated in this study are consistently located about 400m below the surface. GNSS campaign observation from August 2005 to May 2007 detected local ground deformation near the summit of Ontake, and revealed that an inflating source was located about 1km under the area of new fissures. Although the depth of these sources location is not same, the horizontal location of the inflating source detected by GNSS is near the south edge of the deflating source in this study. Moreover, InSAR time-series analysis using ALOS-1 data from 2007 to 2010 revealed that there were displacements meaning inflation near the summit of Ontake and its speed was about 1cm/yr. To discuss the relation between these sources, it is necessary for us to track time-dependent ground deformation in detail and to relocate the source in this study with more precise method, i.e. finite element method, considering the topographic effect to the observed displacements.
Acknowledgements: The ALOS2 data were provided by JAXA. We used RINC software ver.0.36 developed by

Dr. Taku Ozawa at NIED. We also used 10m-DEM provided by the GSI.

Keywords: Ontake, phreatic eruption, volcano deformation

Landform change detected from the airborne laser survey before and after the 2014 Eruption of Ontake Volcano, central Japan

*Takehiko Suzuki[1], Koshun Yamaoka[2], Yoshimichi Senda[3], Souta Unome[3]

1.Faculty of Urban Environmental Sciences, Tokyo Metropolitan University, 2.Earthquake and Volcano Research Center, Graduate School of Environmental Studies, Nagoya University, 3.Nakanihon Air Service

Reconstruction of landform change before and after the eruption is significant in evaluating influence around the volcano. However, it is commonly impossible to survey the landform change directly just after the begging of the eruption by difficulties in access to the area close to the crater. So is the case of the 2014 Eruption of the Ontake Volcano, central Japan. This study aims to clarify the following landform changes by the airborne laser survey conducted in 2005, 2014 (after the eruption) and Sept. 5, 2015, such as fall-out of volcanic ashes, volcanic blocks, landform change around crater, and erosion/ deposition caused by volcanic mud flows.
Positive changes in altitude (Ridge of west Kenga-mine: +0.3–+0.6 m: Near the main craters: +10 m) are concordant of thickness of fall-out ashes shown by previous reports, indicating positive changes in altitude were caused by deposition of ashes. Deposition of ashes with a thickness of +8–+10 m along the valleys just in south slope of west Kenga-mine (Upper reach of Jigoku-dani) suggests passing the pyroclastic flow. This is first quantitative estimation of thickness in this area. This thick sediment filling the valley has disappeared by Sept. 2015, showing occurrence of erosion and transportation. Moreover, this erosion is not only removal of deposited ashes at the eruption but also deeper undercutting for former valley bed with a depth of −4–−6 m, resulting a tendency of erosion in a long term.
On the west slope of Ichino-ike, an uplifted area with 190 m x 35 m stretching WNW-ESE existed just after the eruption. This was most likely formed associated with W1 Crater of the eruption, and is partly composed of mud flow deposit with a thickness of 2–1 m to the maximum. However, it was disappeared by Sept. 2015, probably by the formation of a gully with EW direction.
The most prominent landform change between 2014 and 2015 are erosion/ deposition along valleys (Upper reaches of Shaku-nanzo, Shira, Aka-Jigokudani, Minami-mata, and Yu Rivers) in a wide area. Depth of erosion are −1–−6 m. Beside, positive changes in altitude less than 10 m were recognized in segments with 100 to 500 m long along the Shira and Yu Rivers, indicating depositions. These erosion and deposition are evident in comparison of airborne laser survey data collected in 2015 and 2005, resulting in over undercutting for former valley bed or depositional tendencies in a long term.
We attempted to clarify the distribution of volcanic blocks ejected at the 2014 eruption. However, it was difficult due to precision of data.

Keywords: Airborne laser survey, 2014 Eruption of Ontake Volcano, Landform change

The September 14, 2015 phreatomagmatic eruption of Nakadake crater, Aso Volcano, Japan and its deposits

*Yasuo Miyabuchi[1], Chihoko Hara[1], Yoshiyuki Iizuka[2], Akihiko Yokoo[3]

1.Faculty of Education, Kumamoto University, 2.Institute of Earth Sciences, Academia Sinica, 3.Graduate School of Science, Kyoto University

Following the November 2014-May 2015 magmatic activity including ash and strombolian eruptions, an explosive eruption occurred at Nakadake first crater, Aso Volcano in central Kyushu, southwestern Japan, on September 14, 2015. We performed fieldwork for observing and sampling of the related deposits in the proximal and distal areas immediately after the eruption. Based on these field observations, the eruption deposits were divided into ballistics, pyroclastic density current and ash-fall deposits.
A large number of ballistic clasts was scattered within about 500 m from the center of Nakadake first crater. Although the largest clast with a diameter of 1.6 m existed at the southwestern crater rim, most of ballistic clasts were less than 10 cm in diameter. We sampled all ballistic clasts from an area of 3.5 m^2 at the southwestern rim of Nakadake first crater. The total number of ballistic clasts deposited on the area was 158. Almost half of the ballistics appeared as fresh and unaltered basaltic andesite rocks interpreted to be derived from a fresh batch of magma, while the rest was weakly to highly altered clasts. An area of 2.3 km^2 was covered by a relatively thin ash interpreted to be derived from pyroclastic density currents (PDCs). The deposits were distributed with the SE-trending main axis and two minor axes of the NE and NW. The maximum thickness was less than 10 cm at the crater rim and the PDC deposits were wholly fine grained beds containing no block-sized clasts. Based on the isopach map, the mass of the PDC deposits was estimated at ca. 52,000 tons. The ash-fall deposit was finer grained and was clearly distributed about 8 km to the west of the source crater. The mass of the ash-fall deposit was calculated at about 27,000 tons. Adding the mass of the PDC deposits, the total eruptive mass of the September 14, 2015 event was 79,000 tons.
The polarizing microscope observations revealed that all samples of the September 14 deposits consisted of glass shards (20-30 %), crystal and lithic (40-50 %) grains. Most glass shards were unaltered poorly crystallized pale brown glasses which probably represented juvenile magma. Results of EPMA analysis indicate that chemical composition of glass shards included in the September 14 deposits were similar to those of glasses in the 1979, 1989-1990 and November 2014-May 2015 ash. These evidences including video footages suggest that the September 14, 2015 eruption of Nakadake first crater was phreatomagmatic origin. Similar phreatomagmatic eruptions occurred at Nakadake on September 6, 1979 and April 20, 1990 whose eruptive masses were one order larger than that of September 14, 2015 eruption. These eruptions impose a great hazard for areas within 1-2 km of the active Nakadake crater, yet efficiently impossible to predict due to the lack of any precursors.

Keywords: phreatomagmatic eruption, ballistic clasts, pyroclastic density current, Aso Volcano, Nakadake

Fine sediment discharge after Sep. 14, 2015 Eruption in Aso volcano

*Masayuki Sakagami[1], Masaru Kunitomo[1], Yamato Suzuki[1]

1.National Institute for Land and Infrastructure Management

Nakadake 1st Crater of Aso Volcano in southern Japan erupted on the 14th of September in 2015 where a phreatomagmatic eruptions was occurred and pyroclastic flow was observed, which distributed fine ash deposit around the crater. It is known that fine volcanic ash inducing the infiltration rate lowering, and causes disaster of lahar. Every volcanic eruption, however, may not result in lahar. Therefore, certain criteria is required to evaluate the possibility of a lahar. Survey of sediment deposition was performed three times after the eruption, and particle size was analyzed on the collected samples. In the watersheds around the Nakadake crater, gray mud deposit was detected coating the layer of black volcanic sand. These gray mud deposit consisted of fine particles was not observed at the previous three eruptions between 2014 and 2015. In this presentation, summaries of these observation results will be introduced.

Keywords: Aso-Nakadake Volcano, Lahar, Phreatomagmatic eruption, Pyroclastic flow

Variation of fumarolic gas composition along the volcanic activity of Mt Hakone, Japan

*Takeshi Ohba[1], Muga Yaguchi[1], Ken Ishida[1], Soichiro Kumehara[1], Masahiro yamagishi[1], Yasushi Daita[2]

1.Department of chemistry, School of Science, Tokia University, 2.Hot Spring Res. Inst. Kanagawa Pref.

The driving force of eruption is the degassing of magma or the explosion of hydrothermal reservoir. The volcanic gas contains the component originating in the degassing magma or the hydrothermal reservoir. Therefore, the volcanic gas is essentially important object for the understanding of eruption and the eruptive prediction.
At Mt Hakone, the swarm of volcanic earthquakes has been observed previously. For example, in 2001 the swarm of volcanic earthquakes was observed with the deformation of volcanic body suggesting a pressure source the depth of which was estimated to be 7km (Daita et al, 2009). In parallel to the swarm of earthquakes, the steam pressure in the borehole located in the geothermal area of Owakudani significantly increased. On 26th April 2015, a swarm of volcanic earthquake has started. On 30th June, a small steam eruption took place in the Owakudani geothermal area, which is the first historical eruption at Mt Hakone. The number of earthquake quickly decreased until September of 2015.
Sampling and analysis of fumarolic gas
The Owakudani geothermal area is developed on Mt Kamiyama, one of the central cones of Hakone caldera. The fumarolic gases have been sampled and analyzed at two outlets in Owakudani geothermal area almost every month since May 2013 to Feb 2016. One fumarolic gas (T) is located near the parking of Owakudani geothermal area. Another fumarolic gas (S) is located on the north flank of Mt Kamiyama, 500m far from the fumarole T. The temperature of gas at the outlets was about 96C, which is close to the boiling temperature of the altitude of the fumaroles. The fumarole T associates the discharge of hot spring water. The fumarolic gas was sampled in the evacuated glass bottle containing 20ml of 5M KOH solution. For the determination of SO2/H2S ratio, KIO3-KI solution was reacted with fumarolic gas at the sampling site. For the sampling of condensed water of gas, a double glass tube was used for cooler. The solution in the evacuated glass bottle was analyzed along the method by Ozawa (1968) to determine the amount of H2O, CO2, total S (=H2S + SO2) and R-gas. The R-gas was analyzed by GC with Ar and He carrier gases to determine the relative concentration of He, H2, O2, N2, CH4 and Ar. The isotopic ratio of condensed water was determined by use of an IR-laser cavity ring down analyzer (Picarro).
Result and Discussion
Prior to the small steam eruption on 30th June 2015, definite changes were detected in the composition of fumarolic gas-T. The isotope ratio of H2O (dD) was -51 per mill in Jan 2015. It decreased to -67 per mill on 24th April which was 2 days before the start of earthquake swarm. After the start of earthquake swarm, it increased to -56 per mill on 8th May. Similar to the above change, He/N2 ratio showed precursory change. The ratio was 3.3×10-4 in Dec 2014, followed by the decrease down to 1.1×10-5 on 24th April 2015. The ratio came back to 2.8×10-4 on 8th May. The changes in dD and He/N2 ratio suggest the suppressed supply of magmatic H2O into the shallow hydrothermal system. The suppression might be brought by the development of sealing zone surrounding the degassing magma. The sealing zone is a structure in crust where hydrothermal secondary minerals, such as silica, pyrite, alunite, anhydrite, deposit within the channel of fluid. The deposition of those minerals seals the channel by themselves. If the sealing is complete, the degassing fluid is stored within the sealing zone. The break of the sealing zone episodically injects the magmatic fluid to the shallow hydrothermal system. The increase of fluid

pressure after the injection induced the earthquake swarm stated on 26th April 2015.

Acknowledgments
This study was supported by the Ministry of Education, Culture, Sports, Science and Technology (MEXT) of Japan, under its Earthquake and Volcano Hazards Observation and Research Program.

Keywords: Volcanic gas, Mt Hakone, Magma

Multi-GAS measurements at Mt.Tokachidake

*Risa Okamoto[1], Takeshi Hashimoto[1]

1.Institute of Seismology and Volcanology, Graduate School of Science, Hokkaido University

Introduction: The composition and flux of volcanic gases and those temporal changes are clues to understand degassing processes and their relevant structure below volcanoes.. The system so-called “Multi-GAS” device that consists of several gas sensors has been used to measure the chemical composition of volcanic gases on site (Shinohara, 2005). For the same purpose we started measuring volcanic gases at Mt. Tokachidake and Mt.Tarumae in 2014 using separate portable gas sensors of three kinds. We so far verified that even such a combination of off-the-shelf devices was able to provide reliable results, when applied to the plume with sufficient concentrations (Okamoto, 2015: JpGU).
At Mt.Tokachidake, localized ground inflation near 62-2 crater was detected since 2006 from GNSS by JMA and GSH. During May to August in 2015, further localized acceleration in ground deformation as well as the changes in thermal activity around the crater were found. For example, the fumarolic area called Furikozawa at the south of 62-2 crater extended eastward, whereas the bubbling in the hot ponds was seen at the bottom of 62-2 crater. We repeated our Multi-GAS measurements at Mt. Tokachidake in July and September in 2015 to monitor the temporal changes in gas chemistry associated with the recent volcanic activity.
Field operation: In this study, we used three separate gas sensors (SO_2, H_2S and CO_2). The detection range of each sensor was 0-100 ppm for SO_2, 0-100 ppm for H_2S, 0-9999 ppm for CO_2. The resolution was 1ppm for SO_2, 0.1ppm for H_2S, 1ppm for CO_2. The response time of the CO_2 sensor was approximately one minute, which was considerably longer than the H_2S, SO_2 sensors. For this reason, we walked slowly in the plumes flowing on the crater rims, and took one-minute moving average on the time series of H_2S and SO_2 in order to match them to the CO_2 sensor with the longest time constant. Afterwards, cross-sensitivity between H_2S and SO_2 sensors was calibrated and corrected. At Taisho-vent, due to the prevailing wind and topographic constraint, the plumes were flowing just on the rim. Therefore, we also profiled the gas concentrations to obtain the gas flux.
Results: We measured the plumes from Taisho-vent, 62-2 creator and Furikozawa fumarolic area in July and September in 2015. We obtained almost the same results between the two measurements. Molar ratios between compositions were estimated from the linear trends on the scatter plots as SO_2/H_2S~6, CO_2/H_2S~5 and CO_2/SO_2~1 at Taisho-vent, CO_2/SO_2~0.5 at 62-2 crater, and CO_2/SO_2~0.4 at Furikozawa fumarolic area. Unlike the result from Taisho-vent, H_2S concentrations at 62-2 crater and Furikozawa fumarolic area were close to the detection limit. The SO_2 emission rate was estimated as 6 to 7 t/d. These results were not significantly different from the measurement in 2014 and thus we considered that no essential change in degassing processes took place during this period. Meanwhile, total SO_2 flux (based on the DOAS method) from the crater area in 2015 was reported as 100 to 200 t/d by JMA, which was almost double amount of the flux in 2014. Accordingly, it is likely that most of the SO_2 flux in 2015 was the contribution from 62-2 crater and from the activation of Furikozawa fumaroles. Regarding the difference in gas component between Taisho-vent and others, we have not yet reached any consistent model that can explain all the results above, although we speculate some contribution of the shallow hydrothermal system beneath the crater area.

Keywords: Mt.Tokachidake, volcanic gas

Improvement of the realtime volcano observation system based on the satellite infrared imagery and its application to the case of the 2015 Mt Raung eruption

*Takayuki Kaneko[1], ATSUSHI YASUDA[1], Martin J. Wooster[2], Fukashi Maeno[1]

1.Earthquake Research Institute, University of Tokyo, 2.King's College London

We are monitoring active volcanoes in east Asia using MODIS and MTSAT images. From 2015 through 2017, Japanese new optical satellites, Himawari-8/AHI and GCOM-C/SGLI start operation, which are next generation instruments of the ones we are currently using for monitoring. We plan to replace the MODIS-based realtime thermal monitoring system to a combination system consisting of Himawari-8/AHI and GCOM-C/SGLI. Further, for more precise non-realtime analysis, we also plan to use high-resolution images, in linkage with these two realtime datasets - combined analysis. The new type of Himawari, carrying the AHI sensor, can be used for thermal analysis, because of the improved resolution to be 2km. Also, its ultra-high frequency observation, every 10 minutes, will be particularly useful for thermal analysis of eruption sequences, which can change in a short period. We recently developed a prototype of realtime monitoring system based on Himawari-8/AHI. SGLI onboard GCOM-C is a moderate resolution sensor having resolution of 250m in the 1.6um and 11um channels. The satellite is being launched at the end of 2016 by JAXA. SGLI can be applied for more precise realtime monitoring than MODIS having resolution of 1 km, such as observing enlargement process of lava flows. Here, in non-realtime analysis, high-resolution images are used for specifying topographic change or type and distribution of erupted materials relating to the on-going eruptive process, which cannot be identified by the medium to coarse resolution images. In order to examine effectiveness of the combined analysis based on the three different datasets, we analyzed the 2015 eruption of Raung, as a test case.
Mt Raung, one of the most active volcanoes in Indonesia, is located in the easternmost of Java, Indonesia and has a large conical edifice with altitude of 3320 m. It has a summit caldera of 2km in diameter approximately 300 m in depth, of which topography is similar to the of Miyakejima formed in 2000. In June, 2015, the volcano erupted and lava continued to effuse in the summit caldera from the pyroclastic cone at the center of the floor. Analysis of high-resolution images (Landsat, SPOT, WV and GE) showed that the effused lava enlarged gradually and covered the entire areas of the caldera floor by the middle of July. At the same time, the accumulated lava bed increased in thickness. The total volume of effused lava and the average effusion rate were estimated to be 5.3×10^{7} m^3 and 1.1×10^{6} m^3/day, respectively. We also analyzed Himawari-8/AHI images between 1st of June to 31st of August. The time series variations of thermal anomaly (1.6 um, 2.3 um, 3.9 um) showed that there were two pulses in the activity - Pulse I and II, which were divined by a low activity period at the end of July. Through examining the short term variations, we found that the eruption started at 4:30 on 20th of June (UTC) and ceased on 7th of August. Reactivation of the activity, i.e., start of Pulse II, occurred at 21:10 on 1st of August. The activity level was nearly constant through the majority of the period, which can be considered as a characteristic of the effusive eruption involving Strombolian lava fountaining. Several hours ahead of the onset of Pulse II, a small thermal pulse was observed. This can be a precursor to reactivation of the activity. In substitution for SGLI images, NPOSS/VIIRS images (resolution 380m) were analyzed to observe enlargement process of the lava bed on the caldera floor. We could recognize increase in the size of high-temperature areas at the summit on the 11 um images of VIIRS in the period from late June to early July. This is probably showing enlargement of the lava bed on the caldera floor. This result suggests that we can monitor detailed eruptive phenomena by using SGLI images in realtime. Also, the combined analysis proposed here is considered as a useful method for exploring

eruption sequence.

Keywords: satellite remote sensing, indrared imagery, Indonesia

Estimating the total mass of tephra from radar echo-top height of eruption column

*Keiichi Fukui[1], Eiichi Sato[1], Toshiki Shimbori[1], Kensuke Ishii[1]

1.Meteorological Research Institute

We estimated the total mass of tephra from the time series of echo-top height of eruption cloud detected by the Japan Meteorological Agency radar network. We discussed the relation between the total mass of tephra evaluated by field survey and the total mass estimated from the radar data, and discussed the error in the total mass estimation.

Keywords: total mass of tephra, weather radar, radar echo-top height, eruption column height, estimation of eruptive mass, volcanic ash cloud

The morphology and effusion rate of deep submarine silicic lava flows and domes emplaced during the Havre 2012 eruption, Kermadec Arc, New Zealand

*Fumihiko Ikegami[1], Rebecca J Carey[1], Jocelyn McPhie[1], Adam Soule[2], Kenichiro Tani[3]

1.University of Tasmania, 2.Woods Hole Oceanographic Institution, 3.National Museum of Nature and Science, Japan

1. Introduction
The eruption of Havre 2012 was the largest deep submarine silicic eruption in the modern history (Carey et al. 2014). The eruption was first detected by an airline passenger who saw extensive rafts of floating pumice on the ocean. The later investigation identified the onset of pumice dispersion on the 18th July 2012, which was accompanied by a subaerial plume and hotspot on the NASA MODIS satellite imagery. In addition, significant seismicity at the Havre caldera was measured during this time. Three months after the event, R/V Tangaroa of NIWA (National Institute of Water and Atmospheric Research, New Zealand) visited the Havre volcano and mapped the area using a EM120 multibeam system. This survey detected several new features along the caldera rim which did not exist in 2002. However, the resolution of the map did not permit the identification of the types of volcanic features present.
2. MESH Cruise
In 2014, the Mapping Exploration & Sampling at Havre (MESH) cruise was conducted to visit the seafloor and performed a geological field study of the 2012 eruption deposits. The R/V Roger Revelle (Scripps Institution for Oceanography, UCSD) and two unmanned vehicles, Sentry AUV (Autonomous Underwater Vehicle), and Jason ROV (Remotely Operated Vehicle) of WHOI (Woods Hole Oceanographic Institute) facilitated the voyage. The Sentry AUV mapped the full area of the 5-km wide Havre caldera with high-resolution bathymetry (1-m grid). The ROV Jason conducted traverses along the eruption products discovered by the Sentry high-resolution map, conducting sampling for the rocks and sediments at the seafloor.
3. Results and Discussions
The MESH cruise identified six lava flows (A~D,F,G), eight lava domes (H,I,K~P), two units of ash and lapilli deposits (AL,ABL), two debris avalanche deposit (MF1,2), and an extensively emplaced giant pumice deposit (GP) as the products of the 2012 eruption (Fig. 1). Most of the effusive products which this research focuses on have porphyritic textures with the phenocrysts of plagioclase, and pyroxene. Their whole rock composition ranges from 68~72% SiO2 and inferred that the Havre 2012 magma was rhyodacitic.
The series of lava consists of both lava flows (length of 0.6~1.2 km) and lava domes (height of 70~250 m). Their vents were distributed along the fissures at the southern rim of the caldera which strongly infers structural control for magma ascent. The western part of the fissure is dominated by lava flows (A~G) which immediately descended the 30° slope of the caldera wall. They have clear levee structure with 70~150 m thickness, compression ridges for 10~30 m intervals, and talus with >20 degrees. The fissures from the middle to east formed small lava domes (H~P), although the easternmost one (O-P complex) is exceptionally large (1.1 x 0.8 km elliptical base with 250 m height). The total volume of these effusive products was 0.24 km^3.
The chronology of the lava effusion has been investigated using the stratigraphical relationship to the GP unit, which was dispersed on 18th July. This enables constraints on the lava effusion rate between the 18th July to 19th August (NIWA voyage). The maximum volume of the lava post-dating GP (0.19 km^3 for A, F~P) draws the maximum effusion rate of 25 m^3/s for 90-days average. This values comparable to other well-constrained subaerial silicic lavas, such as 50 m^3/s for 20-days at

Cordon-Caulle 2011 eruption (Bertin et al. 2015), or 66 m^3/s for 14-days at Chaiten 2008 eruption (Pallister et al. 2013).

4. Conclusion

The Havre 2012 eruption produced 0.24 km^3 of rhyodacite lava flows and domes. The largest lava dome grew to the height of 250m and the longest lava flow advanced 1.2km from its vent despite the deep submarine environment. These investigations have calculated submarine silicic lava effusion rates (25 m^3/s) for the first time.

Keywords: Submarine volcano, Submarine caldera, Lava flow morphology, Effusion rate, Rhyolitic magma

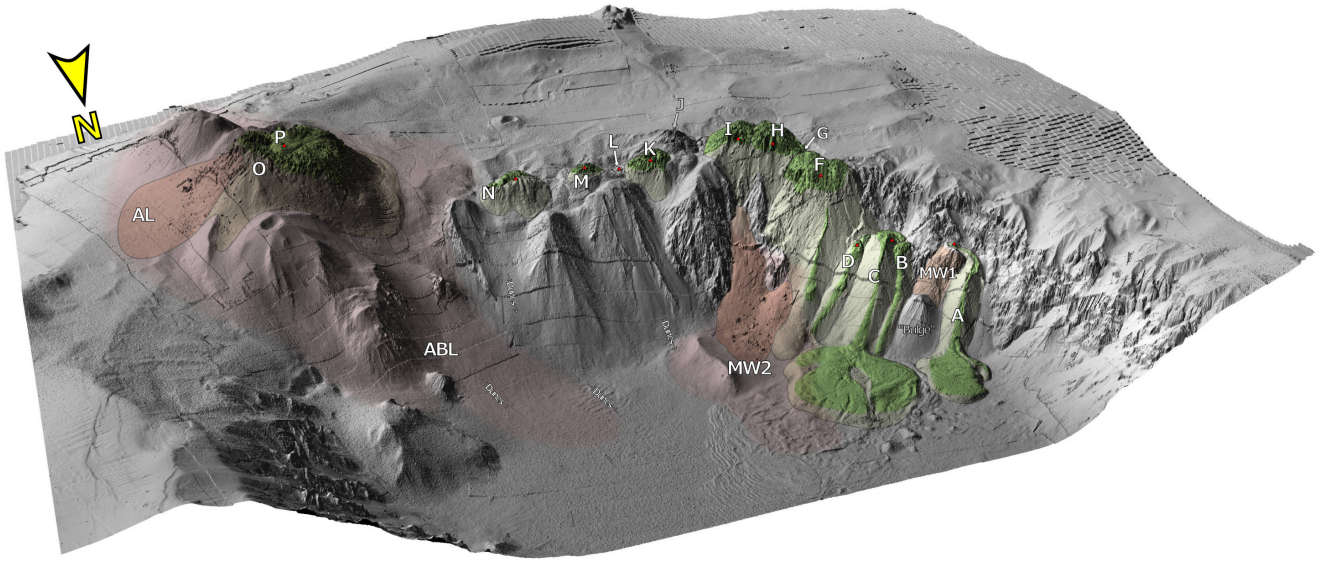

Evolution of magma ascent during the climactic phase of 2011 eruption of Shinmoe-dake, Japan, in view of groundmass microlite textures

*Yuki Suzuki[1], Mie Ichihara[2], Fukashi Maeno[2], Masashi NAGAI[3], Hitomi Shibutani[1], Syouhei Shimizu[1], Setsuya Nakada[2]

1.Department of Earth Sciences, Faculty of Education and Integrated Arts of Sciences, Waseda University, 2.ERI, Univ. of Tokyo, 3.NIED

The climactic phase of the Shinmoe-dake 2011 eruption is characterized by three sub-Plinian events (Jan 26PM, 27AM, 27PM) and a lava accumulation stage in the crater (Jan 27-29), both of which were accompanied by vulcanian events. This study aimed at reconstructing magma ascent in conduit for this phase by using groundmass microlite textures. We then related the changes of magma ascent conditions with those of eruption intensity and style.
The analyzed samples include pumiceous clasts (gray and brown) and denser lava-like juvenile clasts from sub-Plinian (Layer 2-5, each with lower and upper subunits) and Jan 28 vulcanian deposits, and a lava block ejected from the crater on the Feb 1 vulcanian event. These are from magmas of the same chemical and storage conditions just prior to ascent from the reservoir. Representative samples for the textural analyses were selected based on bulk density that reflects syneruptive ascent rate and resultant degree of degassing. Subunits of Layer 2 to Layer 4 resemble one another in bulk density distribution (0.8~1.7 g/cm^3), except Layer3-up with extension to higher density (0.8~2.1 g/cm^3). Also, subunits of Layer 5 to Jan 28 resemble one another (0.8~2.8 g/cm^3) in having extension to much higher density than Layer3-up. The bulk density of Feb 1 lava (2.1g/cm^3) corresponds to high value observed in Layer 5 to Jan 28. The textural analyses were carried out for samples with maximum and minimum bulk densities in representative units (Layer2-up, 3-up, 4-up, 5-low, 5-up, Jan28, Feb 1 Lava).
The crystal size distributions (CSD) of plagioclase microlites are almost the same for all samples over the larger size (40-100 micrometer length in 3D). CSDs over smaller size change depending on the bulk density; dense samples from Layer 5-low, Layer 5-up, Jan 28 and Feb1 lava have steeper CSD than low density samples. These lines of evidence show magma ascent conditions at deeper part of conduit were constant throughout the climactic phase, but condition at shallow part was changing. The higher crystal numbers in dense samples can be explained by either a) higher ascent rate (when undercooling is relatively small, as a whole) or b) lower ascent rate (when undercooling is relatively large). Model b) is more likely in the present case, if decreasing trend of eruption intensity is considered. The bulk density distribution and correlation between bulk density and ascent rate show that the decrease of magma ascent rate at shallow part occurred gradually. The ascent rate variation widened in the third sub-Plinian event (Layer 5), by a little appearance of slowly ascended magmas. Only slowly ascended magmas came to occupy the conduit in the lava accumulation stage.
Suzuki *et al*. (2014 JPGU meeting) proposed that Layer3-up corresponds to the start of the second sub-Plinian event, based on that the bulk density distribution of Layer3-up has an extension to higher density, and degassed magma could have been formed in conduit during the resting phase (Jan 26, 19:00 –Jan 27, 2:00; between the first and second sub-Plinian events) due to decreased eruption rate. The textural study this time newly revealed CSD of plagioclase microlites of high density sample (ca. 2.0 g/cm^3) from Layer3-up resembles those of other pumiceous clasts from the first and second sub-Plinian events, implying conduit residence time of the degassed magma was not extremely long. This interpretation is consistent with the infrasound data indicating quasi-steady state magma flow for the resting phase.

Keywords: Shinmoe-dake, Bulk density, Groundmass microlite, Magma ascent, Degassing, Infrasound

Petrographic study of juvenile blocks of the 1783 A.D. (Agatsuma) pyroclastic flow in Asama Volcano

*Sarina Sugaya[1], Michihiko Nakamura[1], Maya Yasui[2]

1.Department of Earth Sciences, Graduate School of Science, Tohoku University, 2.Department of Geosystem Sciences, College of Humanities and Sciences, Nihon University

The Agatsuma pyroclastic flow (APF) in the 1783 A.D. (Tenmei) eruption of the Asama volcano, central Japan, is characterized by occurrence of abundant rounded juvenile blocks with poorly vesiculated inner core and small proportion of fine ash matrix. The blocks have been referred to as cabbage for their shape and size. APF is a typical example of the "intermediate type" pyroclastic flow defined by Aramaki (1957), which have intermediate characters between the nuée ardente (dome-collapse type) and the pumice flows (column-collapse type) in terms of their volume, density of juvenile blocks and proportion of fine ash matrix. Because these characters may represent the magma outgassing and fragmentation processes, the intermediate type pyroclastic flow may be important to understand key processes that determine the bifurcation between explosive and effusive eruptions. Based on the observation that APF was composed of many (> 50) flow units, Takahashi and Yasui (2013) proposed that APF was generated through fountain collapses following Vulcanian explosions. They also suggested that lava lakes were formed by fall-backs of pyroclasts from the fountains during the Vuclanian activity on the basis of welding structures of the juvenile blocks. However, formation processes of these blocks are unclear. In this presentation, we propose that the cabbage-shaped juvenile blocks were formed repeatedly in the volcanic crater prior to each explosion.
On the surfaces of juvenile blocks ejected at the last stage of the 1783 A.D. eruption, we found the crusts impregnated with very fine (1–10 μm) ash particles and interstitial opal. The presence of opal shows that the juvenile blocks had been emplaced in a hydrothermal system after their rounded shape was formed. Since there is no geothermal area at the sampling location and its upper flank of the Maekake volcano, it is highly possible that silica precipitation from circulated geothermal water followed the formation of characteristic round shape of the juvenile blocks before generation of the APF. The weakly welded ash particles existed between the opal-bearing crust and the inner core; the welding process thus should have occurred before the crust formation. The surfaces of the juvenile blocks without opal-bearing crusts, which were collected from weakly-welded APF deposits, were covered instead with welded ash particles, which may have been formed at the higher temperature condition in the crater. These features indicate that the juvenile blocks were rounded probably via coagulation and welding and coated with volcanic ashes, and filled the crater before their eruption.

Keywords: Asama Volcano, Agatsuma pyroclastic flow, intermediate type pyroclastic flow, opal, welding

